Bioorganic Chemistry 91 (2019) 103127

Contents lists available at ScienceDirect

Bioorganic Chemistry

journal homepage: www.elsevier.com/locate/bioorg

Utilization of tetrahydrobenzo[4,5]thieno[2,3-*d*]pyrimidinone as a cap moiety in design of novel histone deacetylase inhibitors

Mamdouh F.A. Mohamed[a,*], Bahaa G.M. Youssif[b,c], Montaser Sh. A. Shaykoon[d], Mostafa H. Abdelrahman[e], Bakheet E.M. Elsadek[f], Ahmed S. Aboraia[g], Gamal El-Din A. Abuo-Rahma[h,*]

[a] Department of Pharmaceutical Chemistry, Faculty of Pharmacy, Sohag University, 82524 Sohag, Egypt
[b] Department of Pharmaceutical Organic Chemistry, Faculty of Pharmacy, Assiut University, Assiut 71526, Egypt
[c] Department of Pharmaceutical Chemistry, College of Pharmacy, Jouf University, Sakaka 2014, Aljouf, Saudi Arabia
[d] Department of Pharmaceutical Chemistry, Faculty of Pharmacy, Al-Azhar University, 71524 Assiut, Egypt
[e] Department of Pharmaceutical Organic Chemistry, Faculty of Pharmacy, Al-Azhar University, 71524 Assiut, Egypt
[f] Department of Biochemistry, Faculty of Pharmacy, Al-Azhar University, 71524 Assiut, Egypt
[g] Department of Medicinal Chemistry, Faculty of Pharmacy, Assiut University, 71526 Assiut, Egypt
[h] Department of Medicinal Chemistry, Faculty of Pharmacy, Minia University, 61519 Minia, Egypt

ARTICLE INFO

Keywords:
Tetrahydrobenzo[4,5]Thieno[2,3-*d*]pyrimidinone
Histone deacetylase inhibitors
Molecular docking
Anti-proliferative
Apoptotic assay

ABSTRACT

A series of novel 5,6,7,8-Tetrahydro[1]benzothieno[2,3-*d*]pyrimidin-4(3*H*)-one derivatives bearing a hydroxamic acid, 2-aminoanilide and hydrazide moieties as zinc-binding group (ZBG) were designed, synthesized and evaluated for the HDAC inhibition activity and antiproliferative activity. Most of the tested compounds displayed strong to moderate HDAC inhibitory activity. Some of these compounds showed potent anti-proliferative activity against human HepG2, MCF-7 and HCT-116 cell lines. In particular, compounds **IVa**, **IVb**, **IXa** and **IXb** exhibited significant anti-proliferative activity against the three cell lines tested compared to SAHA as a reference. Compound **IVb** is equipotent inhibitor for HDAC1 and HDAC2 as SAHA. It is evident that the presence of free hydroxamic acid group is essential for Zn binding affinity with maximal activity with a linker of aliphatic 6 carbons. Docking study results revealed that compound **IVb** could occupy the HDAC2 binding site and had the potential to exhibit antitumor activity through HDAC inhibition, which merits further investigation.

1. Introduction

Cancer is the most serious disease for humans and it is a leading factor in death worldwide [1]. Apart from the use of radiotherapy and surgery, chemotherapy remains one of the most important choice for treatment of cancer. However, the application of these chemotherapeutic agents is limited by their systemic toxicity, dose-related side effects, lack of selectivity or development of drug-resistance [2]. Consequently, development of effective anticancer agents with enhanced safety profile is the main target for the interested research groups all over the world. Recently, the use of targeted anticancer agents has been proposed as a promising strategy for optimizing antitumor therapies. In particular, histone deacetylases (HDACs) represent one of the most validated cancer targets. Inhibition of histone deacetylases (HDACs) has been proven successful strategy for the development of novel anticancer agents [3]. An aberrant activity of HDACs has been documented in several human cancers leading to development of histone deacetylase inhibitors (HDACIs) [4]. In general, the X-ray structure revealed that the common pharmacophore of HDAC inhibitors consists of 3 parts (Fig. 1): (1) ZBG, a zinc binding group chelating Zinc at the bottom of HDACs active site; (2) a CAP group, interacting with the surface of HDACs; (3) a linker connecting the ZBG and the CAP group [5].

Till now, five HDACIs have been approved by the FDA such as SAHA **(1)**, Romidepsin **(2)**, Belinostat **(3)** and Panobinostat **(4)** [6–10], in addition to chidamide **(5)** which has been approved in 2015 for treatment of PTCL [11] (Fig. 1). Many more HDAC inhibitors, such as compound **(10)** and M344 **(11)**, are in different stages of clinical development for the treatment of hematological malignancies as well as solid tumors. Therefore, developing and identification of potent HDACIs is a promising therapeutic strategy in cancer treatment.

On the other hand, thienopyrimidines, being surrogate and structural analogs of the natural purines, occupy a special position among

* Corresponding authors.
E-mail addresses: mamdouh.fawzi@pharm.sohag.edu.eg (M.F.A. Mohamed), gamal.aborahama@mu.edu.eg (G.E.-D.A. Abuo-Rahma).

https://doi.org/10.1016/j.bioorg.2019.103127
Received 10 December 2018; Received in revised form 6 July 2019; Accepted 15 July 2019
Available online 18 July 2019

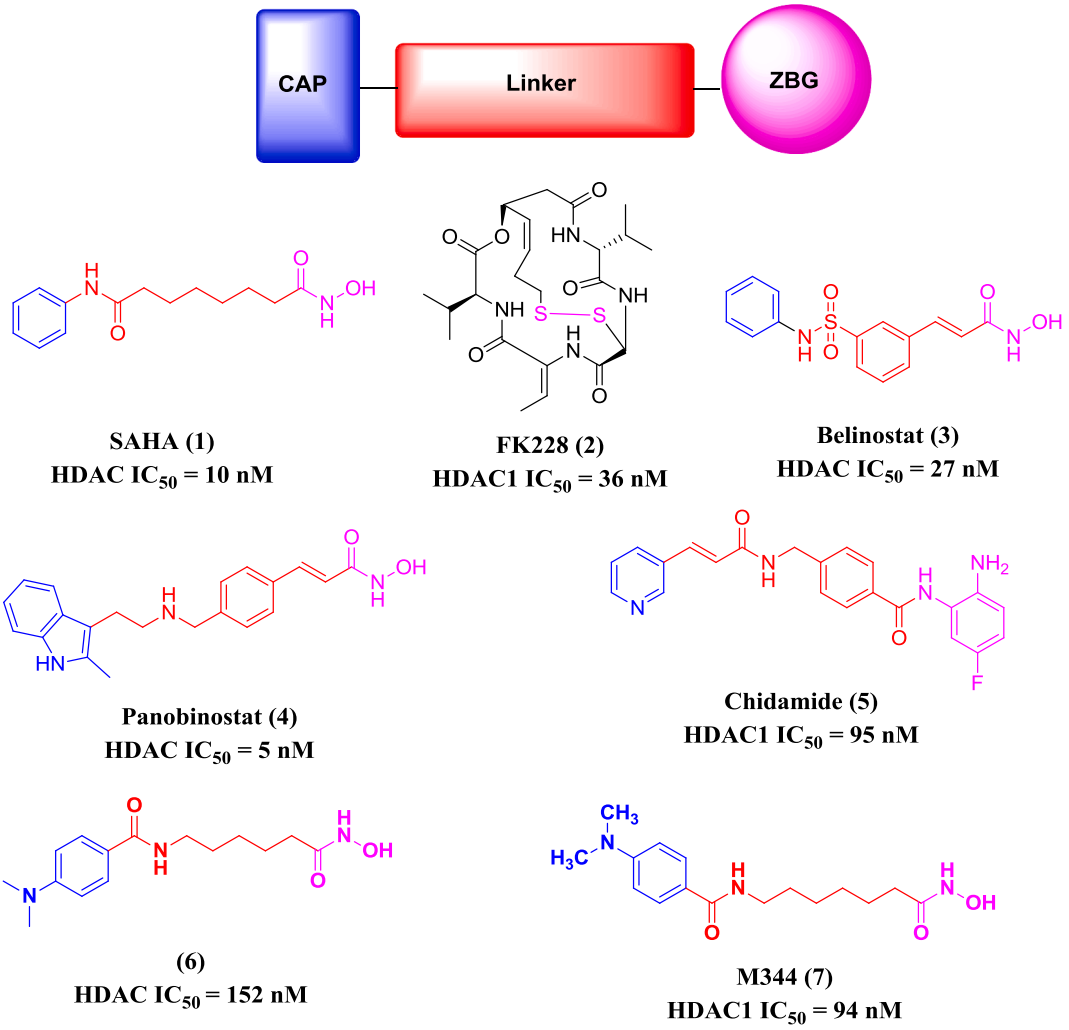

Fig. 1. Structure of HDAC inhibitors.

condensed pyrimidines [12]. Thienopyrimidines derivatives are object of sustained interest due to their vital role in many biological activities such as anti-inflammatory [13,14], antimicrobial [15], analgesic [16,17], anti-cancer [18], blood sugar lowering [16] and CNS depressant [19] activities. Moreover, 5,6,7,8-Tetrahydro[1]benzothieno [2,3-*d*]pyrimidin-4(3*H*)-one derivatives are considered an important sucbclass with significant antitumor activitity [20]. Compound **(8)** is a potent antiproliferative in *P*21 defiecent cancer cells [21]. On the other hand, analogue **(9)** exhibited submicromolar effect in a panel of colon cancer cell lines [18]. Compound **(10)** can induce apoptosis and mitotic catastrophe in apoptosis in colon and ovarian cancer cells [22]. Also, it is believed that the thienopyrimidine scaffold has anticancer activity *via* inhibition of protein kinases. Moreover, Rational modification approach altered a hit from HTS **(11)** [23] to introduce tetrahydropyridothieno[2,3-*d*]pyrimidine derivative **(12)** and **(13)** as highly potent antiproliferative EGFR kinase inhibitors with EGFR IC_{50} = 0.008 and 0.007 μM, respectively [24] (Fig. 2).

Furthermore, in the design of new drugs, the development of hybrid molecules through the combination of different biologically active entities may lead to compounds with interesting biological profiles. In recent years, combination chemotherapy with agents possessing different mechanisms of action is one of the methods that are being adopted to treat cancer. Moreover, a single molecule containing more than one pharmacophore, each with different mode of action could be beneficial for the treatment of cancer [25,26]. Therefore, guided and inspired by the aforementioned information, and in the intensifying efforts to discover new, hopefully more therapeutically efficacious novel HDAC inhibitors, the present work concerns with the synthesis of new Tetrahydrobenzo[4,5]Thieno[2,3-*d*]pyrimidinone/HDACIs hybrids gathering two bioactive entities in one compact structure for increasing the potential anti-tumor effect. The designed hybrids should contain the essential pharmacophores of HDACIs. Tetrahydrobenzo [4,5]Thieno[2,3-*d*]pyrimidinone/HDACIs hybrids, which contain tetrahydrobenzo[4,5]Thieno[2,3-*d*]pyrimidinone as a novel cap group, attached to ZBG *via* aliphatic, aralkyl or aromatic linker (Fig. 3).

The synthesized tetrahydrobenzo[4,5]Thieno[2,3-*d*]pyrimidinone/HDACIs hybrid were evaluated for their HDAC inhibitory activity against HeLa cell nuclear extract. Moreover, the prepared compounds were evaluated for their *in vitro* cytotoxic activity against three human cancer cell lines, HepG2 (hepatocellular carcinoma), MCF-7 (breast carcinoma) and HCT-116 (colon carcinoma) cell lines and structure activity relationship is established.

2. Results and discussion

2.1. Chemistry

The synthetic route of the designated compounds was presented in Schemes 1 and 2. The target compounds **IVa**,**b**, **Va**,**b** and **VIa**,**b** were prepared from the root intermediate **I**. the amino ester **I** was achieved from the low-cost cyclohexanone, element sulfur, and ethyl cyanoacetate *via* Gewald three-components one pot reaction [27] as shown in

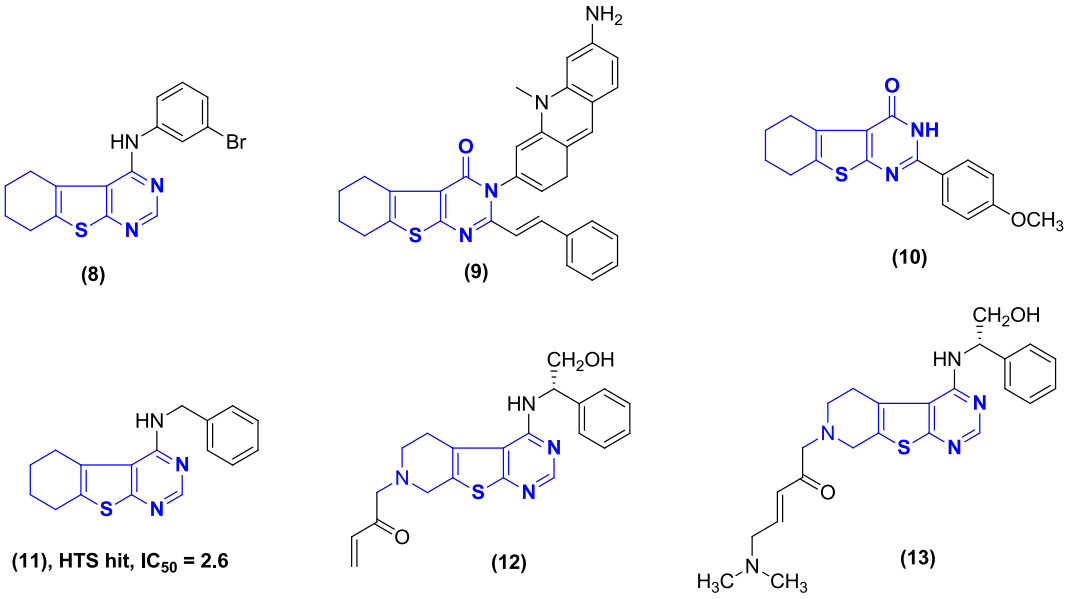

Fig. 2. Structure of anticancer compounds with thienopyrimidine scaffold.

Scheme 1. Compound **II** was synthesized *via* classical cyclocondensation reaction by refluxing the amino ester **I** with formamide to produce the desired compound **II** as pale brown needles [28]. Alkylation of NH group of compound **II** was carried out by heating at reflux of compound **II** with ethyl 6-bromohexanoate or ethyl 7-bromoheptanoate in presence of anhydrous potassium carbonate using acetone as solvent. The resulting ethyl ester underwent acidic hydrolysis with dilute HCl to afford the corresponding acids **IIIa** and **IIIb**. Treating of the appropriate acids **IIIa** and **IIIb** with ethyl chloroformate in the presence of triethylamine as base and acetonitrile as a solvent [29,30] produce the corresponding mixed anhydride. *In situ* reaction of the produced activated acids with hydroxylamine, 1,2-benzenediamine or hydrazine hydrate yielded hydroxamic acids **IVa**,**b**, benzamides **Va**,**b** or hydrazides **VIa**,**b**, respectively as depicted in Scheme 1.

The acylated intermediates **VIIa** and **VIIb** were prepared by reaction of 2-chloroacetyl chloride with 4-aminobenzoic acid or 4-(aminomethyl) benzoic acid in ice-bath using NaOH as a base to afford the desired **VIIa** [31–33], (Scheme 2). heating at reflux compounds **VIIa** and **VIIb** with compound **II** in acetonitrile/water (1:1) in the presence of potassium carbonate followed by acidification yielded the desired compounds **VIIIa** and **VIIIb** as white powder (Scheme 2). Treatment of the corresponding acids **VIIIa** and **VIIIb** with ethyl chloroformate in the presence of triethylamine using THF as a solvent produced the mixed anhydride *in situ*. Reaction of the mixed anhydride with hydroxylamine, 1,2-benzenediamine or hydrazine yielded the hydroxamic acid **IXa,b** the benzamides **Xa,b** and hydrazides **XIa,b** respectively as depicted in Scheme 2.

2.2. Biology

2.2.1. HDAC inhibition activity

In order to explore the HDAC inhibitory activity of the target compounds, all the synthesized compounds were progressed to enzyme inhibition assays against HeLa cell nuclear extract (which contains primarily HDAC1 and HDAC2) with SAHA as positive control [34,35]. The HDAC inhibitory activity of prepared final compounds was measured using Color-de-Lys™ HDAC Colorimetric Assay/Drug Discovery Kit (BML-AK501-0001, Enzo Life Sciences, Inc.) following the protocol provided by the supplier.

Ongoing through the results of *in-vitro* HDAC inhibitory activity of thienopyrimidinone/HDACIs hybrids **IVa**,**b**, **Va**,**b**, **VIa**,**b**, **IXa**,**b**, **Xa**,**b** and **XIa**,**b** (Table 1), it has been observed that compounds bearing the hydroxamic acid as zinc binding group either with aliphatic, aralkyl or aromatic linker possess high potency in HDAC inhibition. Changing the hydroxamic acid group to 2-aminoanilide group or hydrazide group leads to significant decrease in HDAC inhibition activity.

On comparison of results, it has been found that HDAC inhibitory activity of the tested compounds changes on varying the ZBG as follows:

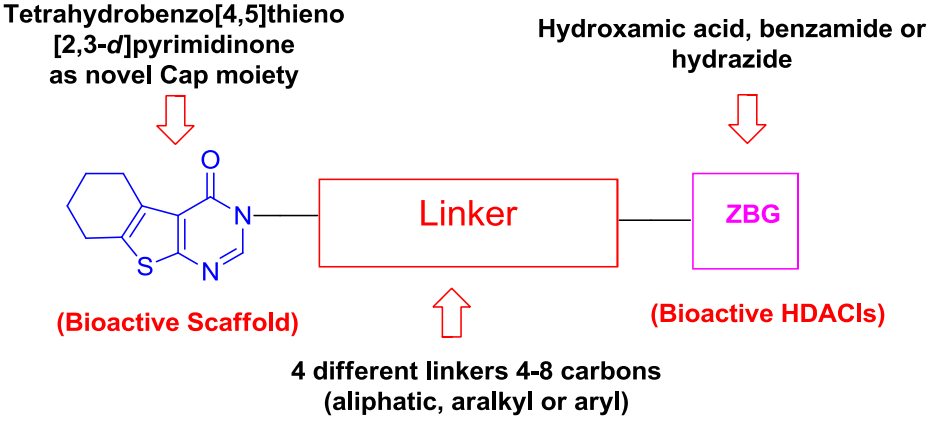

Fig. 3. Design of tetrahydrobenzo[4,5]Thieno[2,3-*d*]pyrimidinone/HDACIs hybrids.

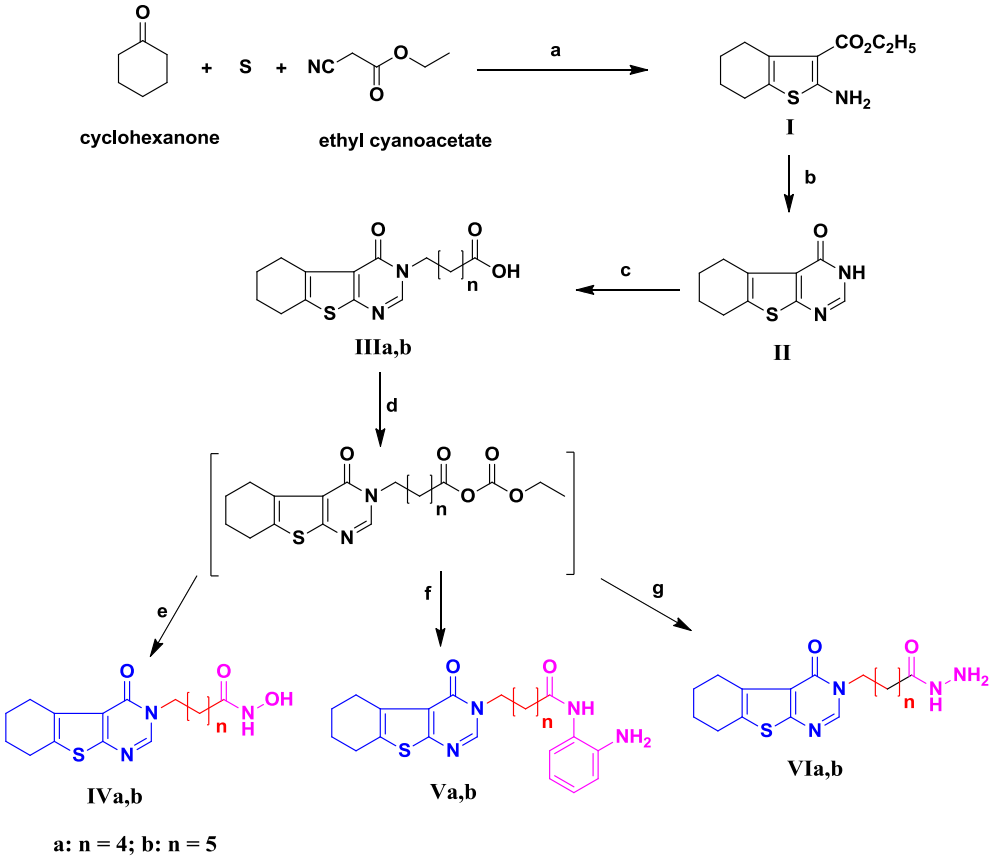

Scheme 1. Synthesis of tetrahydrobenzo[4,5]Thieno[2,3-*d*]pyrimidinone/HDACIs hybrids with aliphatic linker **IVa**,**b**, **Va**,**b** and **VIa**,**b**. **Reagents and reaction conditions** (a) TEA, EtOH, 50 °C, 3h; (b) formamide, reflux; (c) i, appropriate bromo derivatives, K_2CO_3, acetone, reflux, 24h; ii, HCl, reflux; (d) $ClCO_2Et$, CH_3CN, 0–5 °C, 30 min.; (e) NH_2OH, MeOH, rt, 1 h; (f) *o*-phenylenediamine, CH_3CN, rt, overnight; (g) NH_2NH_2, CH_3CN, rt, overnight.

hydroxamic acid > 2-aminoanilide > hydrazide. The *in-vitro* HDAC assay results show that hydroxamic acid-based compounds with aliphatic linker i.e., **IVa** (with an IC_{50} = 0.193 μM) and **IVb** (with an IC_{50} = 0.054 μM) showed greater potency than compounds with aromatic linker i.e., **IXa** and **IXb** in HDAC inhibition. On the other hand, 2-aminoanilide and hydrazide derivatives showed very weak HDAC inhibition activities. Comparing the IC_{50} of the two most potent tetrahydrobenzo[4,5]Thieno[2,3-*d*]pyrimidinone/HDACIs hybrids **IVa**

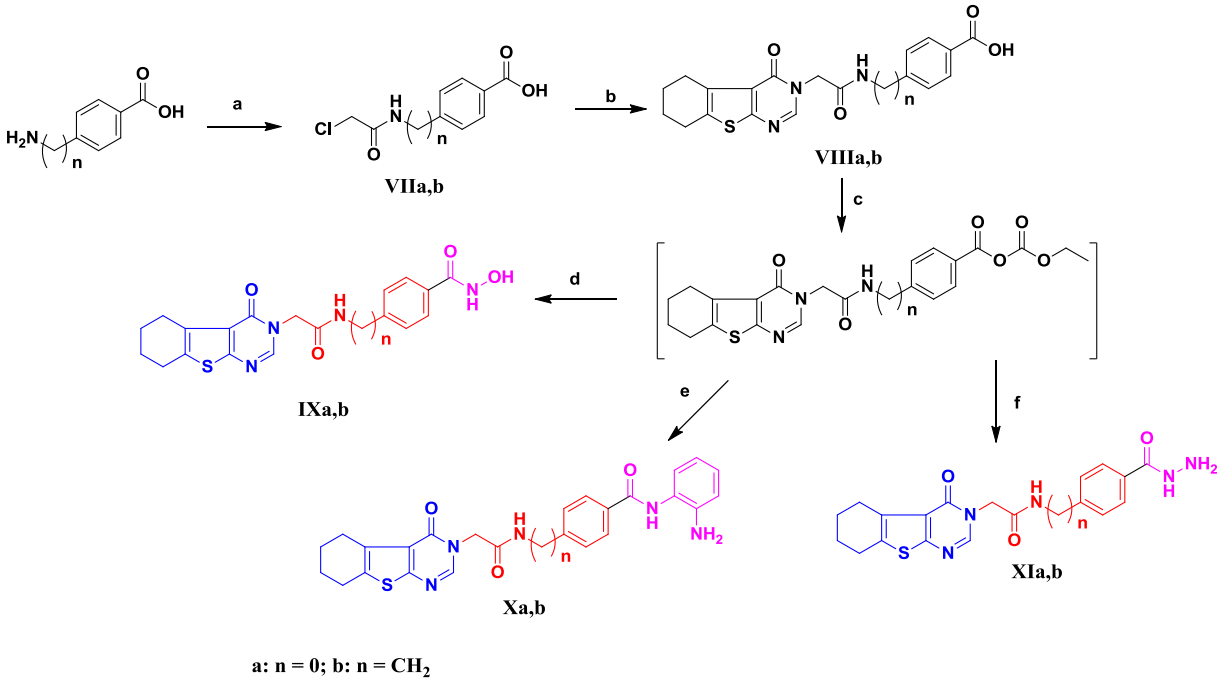

Scheme 2. Synthesis of tetrahydrobenzo[4,5]Thieno[2,3-*d*]pyrimidinone/HDACIs hybrids with aromatic/aralkyl linker **IXa**,**b**, **Xa**,**b** and **XIa**,**b**. **Reagents and reaction conditions** (a) i, chloroacetyl chloride, 2M NaOH; ii, HCl; (b) compound **II**, K_2CO_3, CH_3CN/H_2O (1:1), reflux, overnight; (c) $ClCO_2Et$, CH_3CN, 0–5 °C, 30 min.; (d) NH_2OH, MeOH, rt, 1 h; (e) *o*-phenylenediamine, CH_3CN, rt, overnight; (f) NH_2NH_2, CH_3CN, rt, overnight.

Table 1
HDAC inhibitory activity of the target tetrahydrobenzo[4,5]Thieno[2,3-*d*]pyrimidinone/HDACIs hybrids **IVa,b**, **Va,b**, **VIa,b**, **IXa,b**, **Xa,b** and **XIa,b** on HeLa cell nuclear extract.

Compound	O.D.	Compound	O.D.
IVa	0.087 ± 0.040	**IXa**	0.122 ± 0.040
IVb	0.062 ± 0.053	**IXb**	0.134 ± 0.075
Va	0.207 ± 0.062	**Xa**	0.195 ± 0.072
Vb	0.213 ± 0.065	**Xb**	0.188 ± 0.044
VIa	0.225 ± 0.047	**XIa**	0.233 ± 0.0390
VIb	0.231 ± 0.039	**XIb**	0.224 ± 0.030
Control	0.267 ± 0.092	**SAHA**	0.063 ± 0.024

O.D.: optical density. Data are presented as mean ± SD (n = 3).

and **IVb** with some of the previously published compounds (Fig. 4), it is clear that incorporation of the 5,6,7,8-tetrahydro-3*H*-benzo[4,5]thieno [2,3-*d*] pyrimidin-4-one moiety as a novel cap group represents an important step towards discovering new HDACIs with high potency.

2.2.2. *Anti-proliferative activity*

To investigate the anti-proliferative activity of the tetrahydrobenzo [4,5]Thieno[2,3-*d*]pyrimidinone/HDACIs hybrids, all the synthesized compounds were tested for their anti-proliferative activity by MTT assay method [36] against three human cancer cells HCT-116, MCF-7 and Hep-G2 with the known HDACI, SAHA, as positive control. The results (Table 2, Fig. 5) showed that the tested compounds displayed variable *in-vitro* anticancer activity.

In agreement with the results of the HDAC inhibition activity, the results of antiproliferative activity of the tested compounds revealed that the hydroxamic acid derivatives either with aliphatic or aromatic linker exhibited the highest cytotoxic activity. It was found that the hydroxamic acid derivatives with 5-carbons aliphatic linker **IVa** (with IC_{50} = 3.32 µM, IC_{50} = 4.71 µM, and IC_{50} = 3.36 µM against HCT-116, HepG2, and MCF7 cell lines, respectively) and the hydroxamic acid derivatives with 6-carbons aliphatic linker **IVb** (with IC_{50} = 4.92 µM, IC_{50} = 3.97 µM, and IC_{50} = 4.19 µM against HCT-116, Hep-G2, and MCF7 cell lines, respectively) showed comparable IC_{50} as the reference drug SAHA (with IC_{50} = 1.23 µM, IC_{50} = 3.33 µM, and IC_{50} = 2.18 µM against HCT-116, Hep-G2, and MCF7 cell lines, respectively). The hydrazide derivative **Va** display a good antiproliferative activity against

Table 2
The IC_{50} (µM) of antiproliferative assays of the target tetrahydrobenzo [4,5]Thieno[2,3-*d*]pyrimidinone/HDACIs hybrids **IVa,b**, **Va,b**, **VIa,b**, **IXa,b**, **Xa,b** and **XIa,b**. Data are presented as mean ± SD (n = 3).

Compound	HepG2	HCT-116	MCF-7
IVa	**4.71** ± 0.037	**3.32** ± 0.65	**3.36** ± 0.27
IVb	**3.97** ± 0.92	**4.92** ± 0.41	**4.19** ± 0.032
Va	11.48 ± 0.13	> 100 ± 0.24	9.50 ± 0.12
Vb	70.10	> 100	7.73 ± 0.34
VIa	> 100	> 100	56.06 ± 0.57
VIb	> 100	> 100	78.34 ± 0.13
IXa	**55.79** ± 2.74	**22.24** ± 01.35	**22.72** ± 0.82
IXb	**13.52** ± 3.43	**6.11** ± 0.921	**4.86** ± 0.40
Xa	> 100	> 100	> 100
Xb	> 100	> 100	> 100
XIa	2.26 ± 0.67	15.75 ± 0.26	2.06 ± 0.44
XIb	2.76 ± 1.54	11.04 ± 1.02	2.05 ± 0.58
SAHA	3.33 ± 0.84	1.23 ± 0.27	2.18 ± 0.86

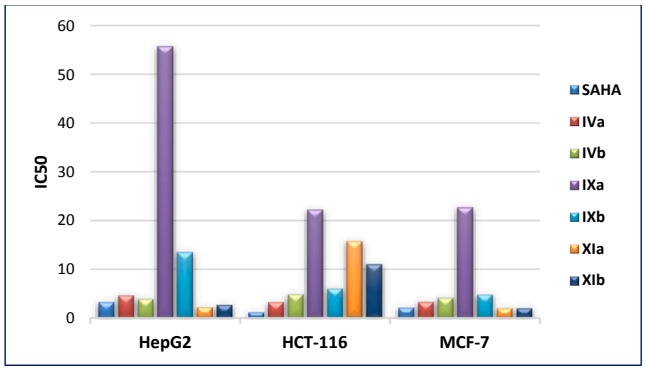

Fig. 5. The IC_{50} (µM) of antiproliferative assays of SAHA and some of target compounds against HCT-116, MCF-7 and Hep-G2 human cancer cell lines.

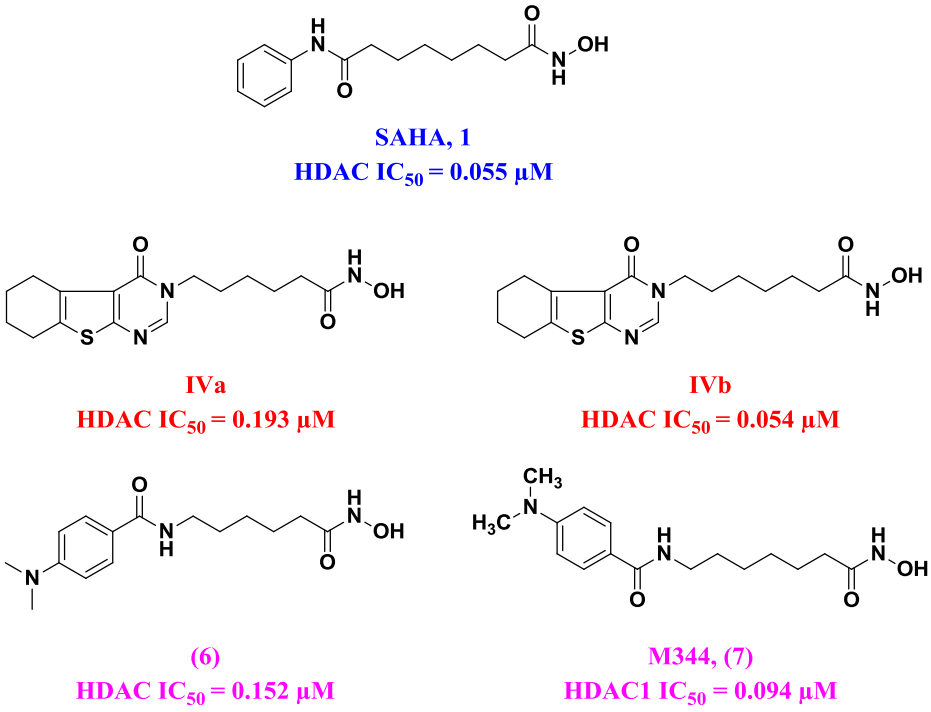

Fig. 4. HDAC IC_{50} of SAHA, **IVa**, **IVb** and some reported compounds.

Hep-G2 and MCF7 cell lines (IC_{50} = 9.50 μM, and IC_{50} = 11.48 μM respectively), but showed weak activity against HCT-116 cell lines (IC_{50} > 100 μM). The hydrazide **Vb** showed a good antiproliferative activity against MCF7 cell lines (IC_{50} = 7.73 μM), but showed weak activity against Hep-G2 and HCT-116 cell lines (IC_{50} > 100 μM). Moreover, among the series containing the aromatic linker **IXa,b, Xa,b** and **XIa,b,** compound **IXb** (with IC_{50} = 6.11 μM, IC_{50} = 13.52 μM, and IC_{50} = 4.86 μM against HCT-116, Hep-G2, and MCF7 cell lines, respectively), **XIa** (with IC_{50} = 15.75 μM, IC_{50} = 2.26 μM, and IC_{50} = 2.10 μM against HCT-116, Hep-G2, and MCF7 cell lines, respectively) and **XIb** (with IC_{50} = 11.04 μM, IC_{50} = 2.76 μM, and IC_{50} = 2.05 μM against HCT-116, Hep-G2, and MCF7 cell lines, respectively) were the most active compounds and the remaining compounds showed weak antiproliferative activity against the three cell lines as shown in Table 2.

From the results, it is obvious that compounds with aliphatic linker and the hydroxamic acid moiety as ZBG showed the highest anti-cancer activity against the three tested cancer cell lines. Changing the aliphatic linker to aralkyl or aryl linker results in decreasing the anti-cancer activity. Moreover, replacement of the hydroxamic acid group with the benzamide group significantly diminishes the anti-cancer activity. It worth noting that, the hydrazide derivatives with aliphatic linker are highly less active than those with aralkyl or aryl linker. The weak HDAC inhibition activity and the high anti-proliferative activity of the hydrazide derivatives with aromatic linker may be attributed to that these derivatives have another mechanism rather than HDAC inhibition.

2.2.3. HDAC isoforms inhibitory activity of representative compounds

In order to explore the HDAC isoform selectivity profile, we chose compounds **IVa** (hydroxamic acid derivatives with 5-carbons aliphatic linker), **IVb** (hydroxamic acid derivatives with 6-carbons aliphatic linker) with most potent HDACs inhibitory activity and **IXa** (hydroxamic acid derivatives with aromatic linker) and **IXb** (hydroxamic acid derivatives with aralkyl linker) to accomplish enzyme inhibitory assays against HDAC1, HDAC2, HDAC6 and HDAC8. Results in Table 3 showed that **IVb** displayed potent preference for HDAC1, HDAC2 and HDAC8 over HDAC6 and the overall selectivity profile of **IVb** was similar to that of SAHA but more potent against HDAC1 and HDAC2 with IC_{50} values of 0.028 μM and 0.078 μM, respectively and that of SAHA 0.031 μM against HDAC1 and 0.081 μM for HDAC2. Moreover, Results showed compound **IVa** demonstrated potent inhibition against HDAC1 and HDAC2, with IC_{50} values of 0.099 μM and 0.220 μM, respectively. By replacing the aliphatic linker ring with aromatic and aralkyl linker respectively, compounds **IXa** and **IXb** showed 7.67 and 6.25 times less potent than compound **IVb** (**IXa**, IC_{50} = 0.215 μM; **IXb**, IC_{50} = 0.175 μM) against HDAC1. Both of **IXa** and **IXb** showed a decreased binding of HDAC2 in comparison with compound **IVb** (3.2-fold and 2.8-fold, respectively). These data demonstrated that aliphatic linker 5 to 6 carbons length is more potent as HDACIs than those of aralkyl or aromatic linker. Eventually, the SAR from this small group of compounds originate compound **IVb** as a potent HDACs inhibitor. The IC_{50} values of compound **IVb** against HDAC1, HDAC2, and HDAC8 was 0.028 μM, 0.078 μM, and 1.903 μM.

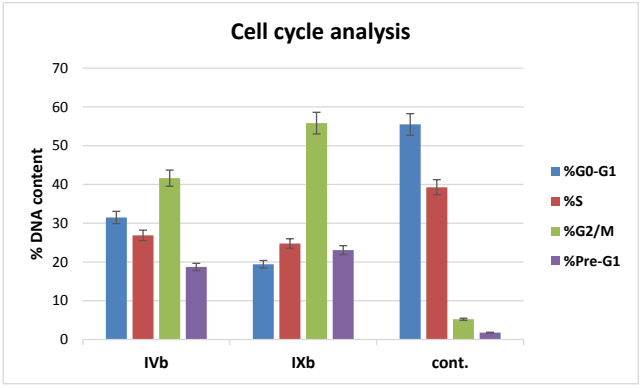

Fig. 6. Cell cycle analysis and apoptosis effect in PC3 cell line treated with **IVb** and **IXb** compounds.

2.2.4. Cell cycle analysis

The cell cycle includes four phases: G1 phase, S phase (synthesis), G2 phase and M phase. During G1, cell amplification and preparation of DNA replication occurs. The S phase is the stage of DNA copying and chromatid duplication. During G2, repairing of new DNA and more growth occurs. In the M stage, nuclear division takes place. Studies on the effect of compounds **IVb** and **IXb** on cell cycle development and induction of apoptosis in the PC3 was done. PC3 was incubated with IC_{50} concentration of compound **IVb** and **IXb** for 24 h. The cell line was stained with PI/Annexin V and analyzed by flow Cytometry using BD FASCC alibur. Investigation of the results (Fig. 6) exposed that percentage of pre G1 apoptosis induced by compound **IVb** on PC3 after 24 h incubation was 18.73%. A high percent of cell accumulation was observed in G2 and M phase in PC3 treated with compound **IVb** after 24 h incubation indicating arrest of cell cycle at G2/M transition. Compound **IXb** on PC3 induced pre G1 apoptosis by 23.06% after 24 h incubation. In addition, PC3 treated with compound **IXb** showed cell accumulation at G2/M phase after 24 h incubation. This indicated that it arrested cell cycle also at G2 phase **(**Fig. 6**,** Table 4**).**

2.2.5. Apoptotic assay

It has been formerly reported that HDACIs can endorse cell apoptosis *in vitro*. Hence, we chose **IVb**, **IXb** to investigate their abilities in inducing cancer cells apoptosis. Cell cycle analysis of PC3 after treatment with compound **IVb** and **IXb**, respectively showed incidence of pre-G1 peak which is a suggestion of apoptosis. To corroborate the ability of both compounds to induce apoptosis, cells were stained with Annexin V/PI, incubated for 24 h and analyzed. Analysis of early and late apoptosis showed that, compounds **IVb** and **IXb** were positively able to make significant levels of apoptosis with necrosis percent 2.71 and 3.23, respectively **(**Fig. 7**,** Table 5**).**

2.3. Molecular docking study

In order to validate our hypothesis, molecular docking studies were carried out for some of the synthesized compounds in the active site **4LXZ** protein. Docking studies have been carried out to explore the

Table 3
HDAC isoforms inhibitory activity of compounds **IVa**, **IVb**, **IXa**, and **IXb**. Data are presented as mean ± SD (n = 3).

		IC_{50}μM			
Compound	HeLa extract	HDAC1	HDAC2	HDAC6	HDAC8
IVa	0.193 ± 0.033	0.099 ± 0.052	0.146 ± 0.036	0.506 ± 0.042	1.315 ± 0.072
IVb	0.054 ± 0.048	0.028 ± 0.049	0.078 ± 0.083	0.471 ± 0.086	1.903 ± 0.056
IXa	0.42 ± 0.062	0.215 ± 0.083	0.250 ± 0.062	2.332 ± 0.075	0.559 ± 0.047
IXb	0.63 ± 0.045	0.175 ± 0.0320	0.220 ± 0.045	1.017 ± 0.053	0.962 ± 0.067
SAHA	0.055 ± 0.069	0.031 ± 0.067	0.081 ± 0.040	0.0334 ± 0.056	1.145 ± 0.044

Table 4
Cell cycle analysis and apoptosis detection of compounds **IVb** and **IXb.**

Compound	%G0-G1	%S	%G2/M	%Pre-G1	Comment
IVb	31.49	26.88	41.63	18.73	PreG1apoptosis and Cell growth arrest at G2/M
IXb	19.42	24.76	55.82	23.06	PreG1apoptosis and Cell growth arrest at G2/M
cont.	55.49	39.27	5.24	1.79	

ability of the synthesized tetrahydrobenzo[4,5]Thieno[2,3-*d*]pyrimidinone/HDACIs hybrids **IVa**, **IVb**, **IXa** and **IXb** to bind to the HDAC2 at the same active site as reported in the literature [37]. Therefore, compound **IVb** (hydroxamic acid derivatives with 6-carbons aliphatic linker) and compound **IXa** (hydroxamic acid derivatives with aromatic linker) were selected for molecular docking studies into the active site of HDAC2 (PDB code: **4LXZ**) using Discovery Studio software package with the aim of elucidating the binding mode of these compounds with HDAC2 and investigate their similarity to the native ligand (SAHA, **1**). Redocking of the known HDAC2 inhibitor Vorinostat (SAHA, **1**) in the

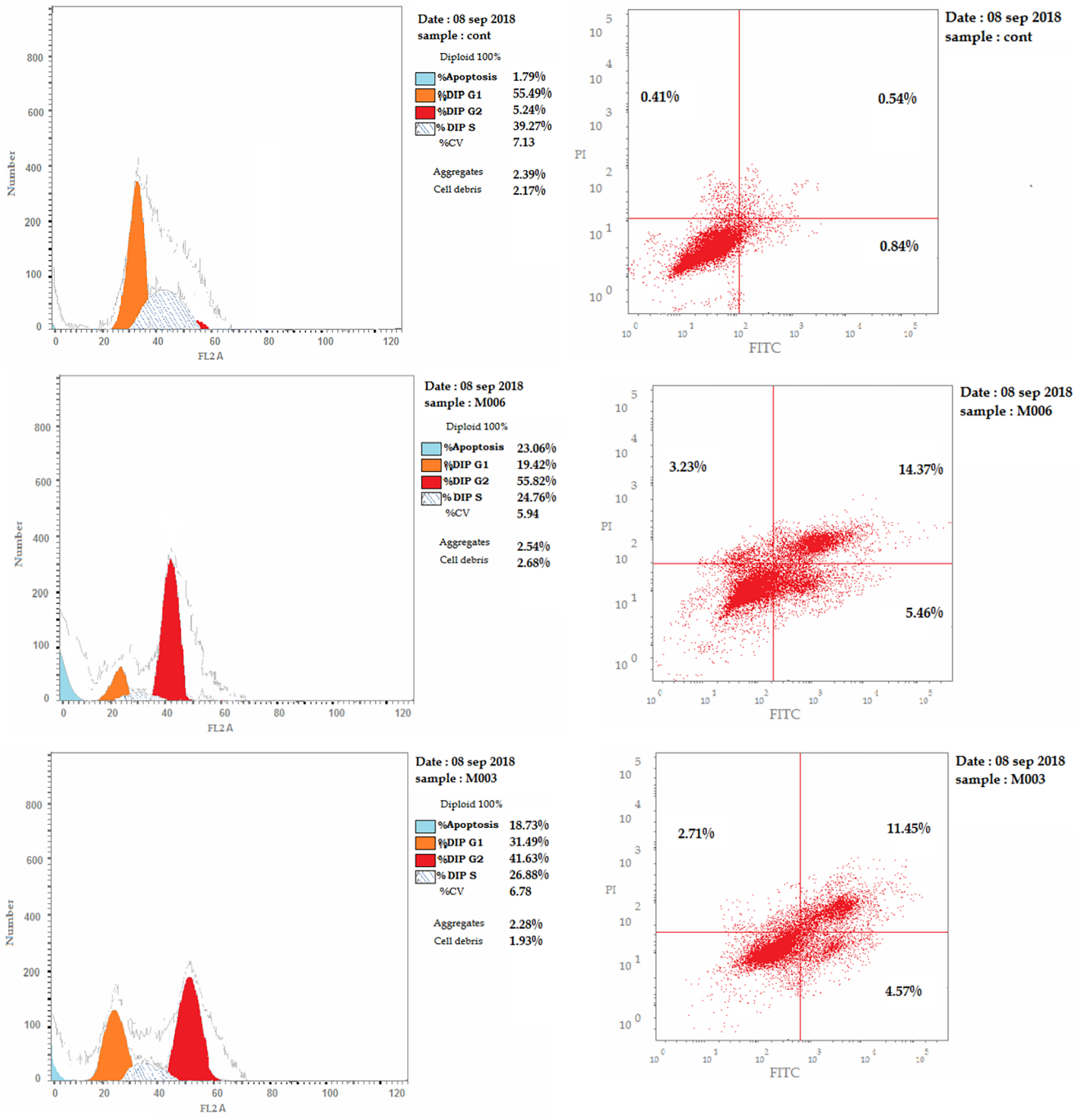

Fig. 7. Cell cycle analysis and Apoptosis induction analysis of compound **IVb** and **IXb** on PC3 cell line.

Table 5
Results of Apoptotic assay of compounds **IVb** and **IXb.**

Compound	Apoptosis			Necrosis
	Total	Early	Late	
IVb	18.73	4.57	11.45	2.71
IXb	23.06	5.46	14.37	3.23
Cont.	1.79	0.84	0.54	0.41

HDAC2 crystal structure (PDB: **4LXZ**) (Fig. 8) showed RMSD value of less than 2 (1.0715) which indicate the confidence in the produced docking results. As shown in Fig. 8, SAHA binds to the active pocket of HDAC2 by forming four hydrogen bonds with amino acid residues His145, His146, Tyr308 and Asp104. In addition to two metallic bonds with the Zn ion and many other hydrophobic interactions with His33 and Pro34 as previously reported indicating our docking method is reliable [37].

Analysis of the docking results revealed that the docking studies were in consistence with the HDAC inhibition assay. From the inspection of the docking results, it was found that compound **IVb** showed comparable CDOCKER energy to the reference ligand and the ZBG interacted with the same amino acids previously reported in molecular modeling studies of SAHA. As shown in Fig. 9**A and B, a** properly positioned ZBG of compound **IVb** was engaged in three hydrogen bonds with amino acid residues His145, His146 and Tyr308. In addition to two metallic bonds with the Zn ion and hydrophobic interactions with His 33.

On the other hand, compound **IXa**, occupied the HDAC2-binding pocket (Fig. 9**C and D**) with engaging in hydrogen bonding with different amino acid residues within the vicinity of the binding pocket, including: His146, His183 and Gly154. In addition, one metal bond with Zn:401 and show hydrophobic interaction with the different residues within the pocket include; His33, Asp104, Phe155 and Phe210. Based on the docking results above, as a promising novel HDACIs agent, compound **IVb** could occupy the HDAC2 binding site and had the potential to exhibit antitumor activity through HDAC inhibition, which merits further investigation.

3. Conclusion

In summary, 12 new final compounds were synthesized, characterized and progressed to enzyme inhibition assay against HeLa cell nuclear extract and their anti-cancer potency against three human cancer cell lines (HCT-116, MCF-7, HepG2) by MTT method with SAHA as positive control. Among the tested compounds, the hydroxamic acid derivatives with aliphatic, aralkyl or aromatic linker were the most potent and that compounds **IVa** and **IVb** could be considered as promising candidates for the future development of the treatment of cancer. Tetrahydrobenzo[4,5]Thieno[2,3-*d*]pyrimidinone is a promising cap moiety. Aliphatic linker 5 to 6 carbons length is more potent as HDACIs than those of Aralkyl or aromatic linker. Hydroxamic acid is the most potent, replacement of Hydroxamic acid group with benzamide or hydrazide strongly decrease the HDAC inhibition activity. Compound **IVb** exhibited inhibitory activity for HDAC1 and HDAC2 equipotent to SAHA with IC_{50} value of 0.028 μM and 0.078 μM, respectively. Cell cycle analysis data and apoptosis detection investigation for **IVa** and **IXb** proved that these two compounds can arrest cell cycle at G2/M phase and to make significant levels of apoptosis with necrosis percent of 2.71 and 2.23, respectively. Therefore, hybrid derivatives **IVa** and **IVb** are promising lead compounds that had strong potential to be further developed as novel HDACIs. Further structural optimization of these promising anticancer agents especially is ongoing for more precise SAR information and agents that are more potent.

4. Experimental section

4.1. Chemistry

Melting points were determined on an electrothermal melting point apparatus (Stuart Scientific Co.) and were uncorrected. IR spectra are recorded as KBr disks on a Shimaduz 408 instrument Spectrophotometer at the Faculty of Science, Sohag University. NMR Spectra were taken on the Varian Unity INOVA 400 MHz spectrometers for proton and carbon at Aberdeen University, U.K. All numbers referring to NMR data obtained are in parts per million (ppm). LCMS spectrometric data were obtained using the Thermo Instruments MS system (LTQ XL/LTQ Orbitrap Discovery) coupled to a Thermo Instruments HPLC system (Accela PDA detector, Accela PDA auto sampler and Pump) at Aberdeen University, U.K. For TLC, the DC Alufolien, Kieselgel 60 F_{254} precoated plates are used (Merck, Darmstadt, Germany). Ethyl 2-amino-4,5,6,7-Tetrahydrobenzo[*b*]thiophene-3-carboxylate **I** [38], 5,6,7,8-Tetrahydro-3*H*-benzo[4,5]thieno[2,3-*d*]pyrimidin-4-one **II** [28], 4-(2-chloroacetamido) benzoic acid **VIIa** and 4-[(2-chloroacetamido)methyl] benzoic acid **VIIb** [33] were prepared according to reported procedures.

4.1.1. *General procedure for the synthesis of 6-(4-Oxo-5,6,7,8-Tetrahydro-3H-benzo[4,5]thieno[2,3-d] pyrimidin-3-yl)alkanoic acid IIIa and IIIb*

A mixture of compound **II** (2.06 g, 10 mmol), ethyl-6-bromohexanoate or ethyl-7-bromoheptanoate (10 mmol) and anhydrous

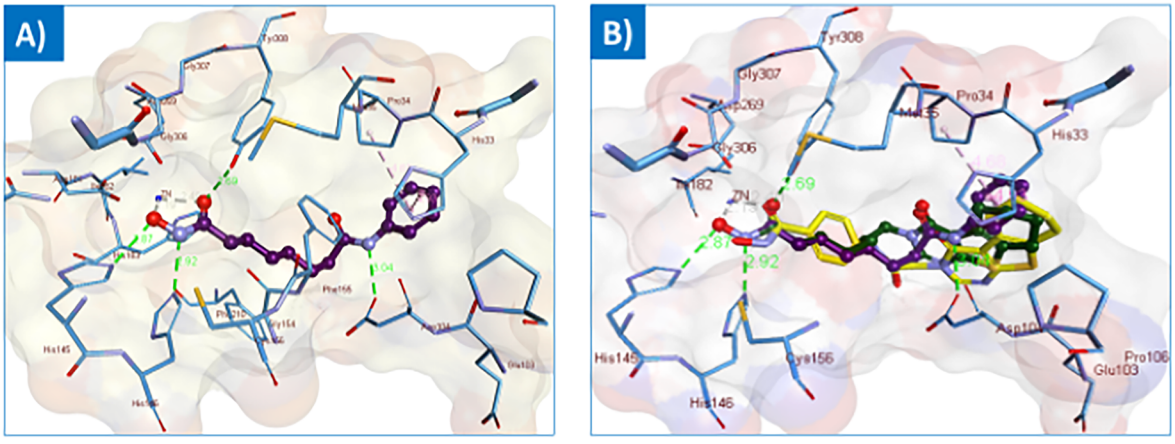

Fig. 8. Docking and binding pattern of compound **SAHA** (magenta) into the active site of HDAC2 (PDB: 4LXZ) 3D structure (B) The superimposition of the docked poses **IVb** (green), **IXa** (yellow) and the co-crystallized **SAHA** (magenta) into the active site of HDAC2 (PDB: 4LXZ). Dashed green lines represent hydrogen bonds.

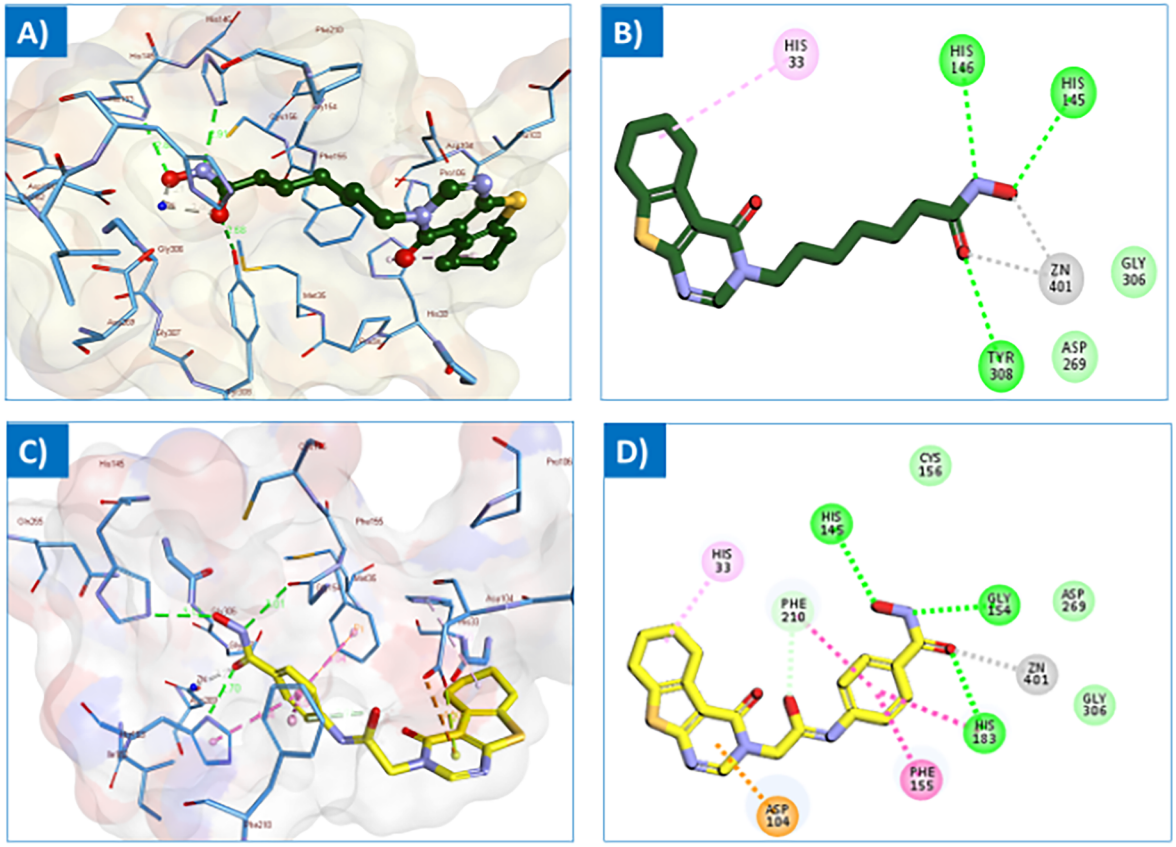

Fig. 9. Docking and binding pattern of the top docking poses into the active site of HDAC2 (PDB: 4LXZ) **(A)** 3D structure of compound **IVb** (green) **(B)** 2D structure compound **IVb (C)** 3D structure compound **IXa** (yellow) **(D)** 2D structure compound **IXa**. All hydrogens were removed for the purposes of clarity.

potassium carbonate (5.52 g, 40 mmol) in dry acetone (30 mL) heated at reflux for 24 h. The reaction mixture was cooled, the formed precipitate was filtered and the filtrate was evaporated under reduced pressure. The obtained oil residue was heated with 2 N HCl (10 mL) at 75 °C for 3 h. Upon cooling, the formed precipitated solid was filtered off, dried and recrystallized from acetone to give **IIIa** and **IIIb** as white needles.

4.1.1.1. ***6-(4-Oxo-5,6,7,8-Tetrahydro-3H-benzo[4,5]thieno[2,3-d] pyrimidin-3-yl) hexanoic acid (IIIa)***. White needles, (2.23 g, 69.5% yield); mp: 138–140 °C; IR (KBr, cm^{-1}): 3157–2499 (OH), 1732 (C=O), 1678 (C-4, C=O) cm^{-1}; ^{1}H NMR (400 MHz, $CDCl_3$) δ (ppm): 7.91 (s, 1H, Ar-H), 3.97 (t, 2H, J = 8 Hz, N−CH_2), 3.02 (t, 2H, J = 6 Hz, CH_2), 2.77 (t, 2H, J = 8 Hz, CH_2), 2.37 (t, 2H, J = 8 Hz, CH_2CO), 1.93–1.73 (m, 6H, 3 CH_2), 1.73–1.65 (m, 2H, CH_2), 1.47–1.39 (m, 2H, CH_2); ^{13}C NMR (100 MHz, $CDCl_3$) δ (ppm): 178.46, 161.98, 157.94, 145.67, 134.37, 131.75, 122.99, 46.59, 33.77, 29.31, 26.16, 25.79, 25.40, 24.25, 23.02, 22.40; HRMS *m/z* calcd for $[M+H]^+$ $C_{16}H_{20}N_2O_3S$: 321.1267, found: 321.1261.

4.1.1.2. ***7-(4-Oxo-5,6,7,8-Tetrahydro-3H-benzo[4,5]thieno[2,3-d] pyrimidin-3-yl) heptanoic acid (IIIb)***. White needles, (2.24 g, 67% yield); mp: 130–132 °C; IR (KBr, cm^{-1}): 3154–2490 (OH), 1718 (C=O), 1667 (C-4, C=O) cm^{-1}; ^{1}H NMR (400 MHz, $CDCl_3$) δ (ppm): 7.90 (s, 1H, Ar-H), 3.95 (t, 2H, J = 6, N−CH_2), 3.02 (t, 2H, J = 6 Hz, CH_2), 2.77 (t, 2H, J = 8 Hz, CH_2), 2.35 (t, 2H, J = 8 Hz, CH_2CO), 1.89–1.74 (m, 6H, 3 CH_2), 1.68–161 (m, 2H, CH_2), 1.42–1.37 (m, 4H, 2 CH_2); ^{13}C NMR (100 MHz, $CDCl_3$) δ (ppm): 178.72, 162.01, 157.96, 145.66, 134.33, 131.76, 122.99, 46.73, 33.86, 29.50, 28.67, 26.43, 25.80, 25.40, 24.60, 23.03, 22.41; HRMS *m/z* calcd for $[M+H]^+$ $C_{17}H_{23}N_2O_3S$: 335.1424, found: 335.1415.

4.1.2. ***General procedure for the synthesis of N-Hydroxy-6-(4-oxo-5,6,7,8-Tetrahydro-3H-benzo[4,5]thieno [2,3-d]pyrimidin-3-yl) alkanamide IVa and IVb***

To a solution of compound **IIIa** or **IIIb** (2.5 mmol) in acetonitrile (30 mL), Et_3N (0.87 mL, 6.25 mmol) was added. The solution was cooled to 0–5 °C, then $ClCO_2C_2H_5$ (0.28 mL, 3 mmol) was added dropwise into the solution and the reaction mixture was stirred at 0–5 °C for 30 min. The reaction mixture was filtered off and the filtrate was dropped into a freshly prepared solution of NH_2OH (1.74 g, 25 mmol) in methanol (10 mL). After stirring at room temperature for 1 h, water was added to the reaction mixture and the precipitated solid was filtered off, washed with water and dried and recrystallized from ethanol to afford compounds **IVa** and **IVb**.

4.1.2.1. ***N-Hydroxy-6-(4-oxo-5,6,7,8-Tetrahydro-3H-benzo[4,5] thieno[2,3-d] pyrimidin-3-yl)hexanamide (IVa)***. White crystals, (0.47 g, 59% yield); mp: 175–177 °C; IR (KBr, cm^{-1}): 3251 (NHOH), 1650 (C=O) cm^{-1}; ^{1}H NMR (400 MHz, $CDCl_3$) δ (ppm): 10.32 (s, 1H, NH), 8.66 (s, 1H, OH), 8.32 (s, 1H, Ar-H), 3.91 (t, 2H, J = 8 Hz, N−CH_2), 2.88 (t, 2H J = 8 Hz, CH_2), 2.73 (t, 2H, J = 8 Hz, CH_2), 1.94 (t, 2H, J = 8 Hz, CH_2CO), 1.82–1.73 (m, 4H, 2 CH_2), 1.68–1.60 (m, 2H, CH_2), 1.55–1.48 (m, 2H, CH_2), 1.28–1.21 (m, 2H, CH_2); ^{13}C NMR (100 MHz, $CDCl_3$) δ (ppm): 168.93, 161.47, 156.91, 147.43, 132.78, 130.80, 121.74, 45.37, 32.06, 28.54, 25.56, 25.37, 24.67, 24.54, 22.39, 21.77; HRMS *m/z* calcd for $[M+H]^+$ $C_{16}H_{22}N_3O_3S$: 336.1376, found: 336.1371.

4.1.2.2. ***N-Hydroxy-7-(4-oxo-5,6,7,8-Tetrahydro-3H-benzo[4,5] thieno[2,3-d] pyrimidin-3-yl)heptanamide (IVb)***. White needles, (0.63 g, 75% yield); mp: 176–178 °C; IR (KBr, cm^{-1}): 3256 (NHOH), 1648 (C=O) cm^{-1}; ^{1}H NMR (400 MHz, $CDCl_3$) δ (ppm): 10.32 (s, 1H, NH), 8.65 (s, 1H, OH), 8.30 (s, 1H, Ar-H), 3.90 (t, 2H, J = 8 Hz,

N−CH_2), 2.87 (t, 2H, J = 8 Hz, CH_2), 2.72 (t, 2H, J = 8 Hz, CH_2), 1.92 (t, 2H, J = 8 Hz, CH_2CO), 1.83–1.68 (m, 4H, 2 CH_2), 1.66–1.61 (m, 2H, CH_2), 1.49–1.45 (m, 2H, CH_2), 1.29–1.21 (m, 4H, 2 CH_2); ^{13}C NMR (100 MHz, $CDCl_3$) δ (ppm): 169.04, 161.48, 156.90, 147.41, 132.75, 130.80, 121.74, 45.48, 32.16, 28.70, 28.16, 25.73, 25.37, 24.99, 24.54, 22.39, 21.77; HRMS *m/z* calcd for $[M+H]^+$ $C_{17}H_{24}N_3O_3S$: 350.1533, found: 350.1526.

4.1.3. *General procedure for the synthesis of N-(2-Aminophenyl)-6-(4-oxo-5,6,7,8-Tetrahydro-3H-benzo[4,5]thieno[2,3-d]pyrimidin-3-yl)alkanamide Va and Vb*

To a solution of compound **IIIa** or **IIIb** (2.5 mmol) in acetonitrile (30 mL), Et_3N (0.87 mL, 6.25 mmol) was added. After cooling the reaction mixture to 0–5 °C, $ClCO_2C_2H_5$ (0.28 mL, 3 mmol) was added dropwise with stirring at 0–5 °C for 30 min. The reaction mixture was filtered and the filtrate was dropped into a solution of *o*-phenylenediamine (2.23 g, 20.62 mmol) in acetonitrile. After overnight stirring at room temperature, the reaction mixture was quenched with water and the resulting precipitate was filtered off, washed with water, ethanol and dried, followed by recrystallization from ethanol to afford **Va** and **Vb**.

4.1.3.1. *N-(2-Aminophenyl)-6-(4-oxo-5,6,7,8-Tetrahydro-3H-benzo[4,5]thieno-[2,3-d]pyrimidin-3-yl)hexanamide (Va)*. White powder, (0.75 g, 73% yield); mp: 181–182 °C; IR (KBr, cm^{-1}): 3462, 3369, 3354 (NH, NH_2), 1654 (C═O) cm^{-1}; ^{1}H NMR (400 MHz, $CDCl_3$) δ (ppm): 7.88 (s, 1H, Ar-H), 7.43 (s, 1H, NH), 7.16 (d, 1H, J = 8 Hz, Ar-H), 7.04 (t, 1H, J = 8 Hz, Ar-H), 6.78–6.72 (m, 2H, Ar-H), 3.96 (t, 2H, J = 8 Hz, N−CH_2), 3.88 (s, 2H, NH_2), 2.99 (t, 2H, J = 8 Hz, CH_2), 2.77 (t, 2H, J = 8 Hz, CH_2), 2.40 (t, 2H, J = 8 Hz, CH_2CO), 1.89–1.76 (m, 8H, 4 CH_2), 1.50–1.44 (m, 2H, CH_2);^{13}C NMR (100 MHz, $CDCl_3$) δ (ppm): 171.53, 162.30, 158.04, 145.56, 140.88, 134.36, 131.68, 127.22, 125.29, 124.50, 122.94, 119.60, 118.33, 46.45, 36.53, 29.18, 26.09, 25.81, 25.39, 25.09, 23.00, 22.39; HRMS *m/z* calcd for $[M+H]^+$ $C_{22}H_{27}N_4O_2S$: 411.1849, found: 411.1844.

4.1.3.2. *N-(2-Aminophenyl)-7-(4-oxo-5,6,7,8-Tetrahydro-3H-benzo[4,5]thieno [2,3-d]pyrimidin-3-yl)heptanamide (Vb)*. White powder, (0.57 g, 54% yield); mp: 141–143 °C; IR (KBr, cm^{-1}): 3451, 3373, 3238, 3354 (NH, NH_2), 1654 (C═O) cm^{-1}; ^{1}H NMR (400 MHz, $CDCl_3$) δ (ppm): 7.87 (s, 1H, Ar-H), 7.47 (s, 1H, NH), 7.16 (d, 1H, J = 8 Hz, Ar-H), 7.03 (t, 1H, J = 8 Hz, Ar-H), 6.78–6.72 (m, 2H, Ar-H), 3.95 (t, 2H, J = 8 Hz, N−CH_2), 3.87 (s, 2H, NH_2), 3.00 (t, 2H, J = 8 Hz, CH_2), 2.77 (t, 2H, J = 8 Hz, CH_2), 2.37 (t, 2H, J = 8 Hz, CH_2CO), 1.90–1.70 (m, 8H, 4 CH_2), 1.48–1.27 (m, 4H, 2 CH_2); ^{13}C NMR (100 MHz, $CDCl_3$) δ (ppm): 171.78, 162.24, 158.02, 145.57, 140.95, 134.32, 131.68, 127.21, 125.33, 124.52, 122.93, 119.55, 118.30, 46.44, 36.76, 29.49, 28.60, 26.28, 25.82, 25.58, 25.38, 23.00, 22.39; HRMS *m/z* calcd for $[M+H]^+$ $C_{23}H_{29}N_4O_2S$: 425.2006, found: 425.1995.

4.1.4. *General procedure for the synthesis of 6-(4-Oxo-5,6,7,8-Tetrahydro-3H-benzo[4,5]thieno[2,3-d] pyrimidin-3-yl)hexanoic acid hydrazide VIa and VIb*

To a solution of compound **IIIa** or **IIIb** (2.5 mmol) in acetonitrile (30 mL), Et_3N (0.87 mL, 6.25 mmol) was added. After cooling the reaction mixture to 0–5 °C, $ClCO_2C_2H_5$ (0.28 mL, 3 mmol) was added dropwise and the reaction mixture was stirred for further 30 min at 0–5 °C. The reaction mixture was filtered and the filtrate was dropped into a solution of hydrazine (0.5 mL, 10 mmol) in acetonitrile. After overnight stirring at room temperature, the reaction mixture was quenched with water and the separated solid was filtered off, washed with water and ethanol. The crude product was crystallized from ethanol to afford the target compounds **VIa** and **VIb**.

4.1.4.1. *6-(4-Oxo-5,6,7,8-Tetrahydro-3H-benzo[4,5]thieno[2,3-d] pyrimidin-3-yl) hexanoic acid hydrazide (VIa)*. White powder, (0.60 g, 72% yield); mp: 170–172 °C; IR (KBr, cm^{-1}): 3337, 3283, 3354 (NH, NH_2), 1658 (C═O) cm^{-1}; ^{1}H NMR (400 MHz, DMSO-d_6) δ (ppm): 8.91 (s, 1H, NH), 8.32 (s, 1H, Ar-H), 4.14 (s, 2H, NH_2), 3.91 (t, 2H, J = 8 Hz, N−CH_2), 2.88 (t, 2H, J = 8 Hz, CH_2), 2.74 (t, 2H, J = 8 Hz, CH_2), 2.01 (t, 2H, J = 8 Hz, CH_2CO), 1.84–1.70 (m, 4H, 2 CH_2), 1.70–1.58 (m, 2H, CH_2), 1.54–148 (m, 2H, CH_2), 1.31–1.18 (m, 2H, CH_2); ^{13}C NMR (100 MHz, DMSO-d_6) δ (ppm): 171.43, 161.47, 156.91, 147.44, 132.77, 130.80, 121.74, 45.37, 33.21, 28.54, 25.60, 25.37, 24.77, 24.54, 22.39, 21.77; HRMS *m/z* calcd for $[M+H]^+$ $C_{16}H_{23}N_4O_2S$: 335.1536, found: 335.1530.

4.1.4.2. *7-(4-Oxo-5,6,7,8-Tetrahydro-3H-benzo[4,5]thieno[2,3-d] pyrimidin-3-yl) heptanoic acid hydrazide (VIb)*. Pale brown flakes, (0.76 g, 87% yield); mp: 139–140 °C IR (KBr, cm^{-1}): 3334, 3277, 3354 (NH, NH_2), 1655 (C═O) cm^{-1}; ^{1}H NMR (400 MHz, DMSO-d_6) δ (ppm): 8.90 (s, 1H, NH), 8.31 (s, 1H, Ar-H), 4.13 (s, 2H, NH_2), 3.90 (t, 2H, J = 8 Hz, N−CH_2), 2.87 (t, 2H, J = 8 Hz, CH_2), 2.72 (t, 2H, J = 8 Hz, CH_2), 1.99 (t, J = 8 Hz, CH_2CO), 1.80–1.73 (m, 4H, 2 CH_2), 1.63–1.61 (m, 2H, CH_2), 1.49–1.46 (m, 2H, CH_2), 1.27–1.21 (m, 4H, 2 CH_2); ^{13}C NMR (100 MHz, DMSO-d_6) δ (ppm):171.54, 161.47, 156.90, 147.41, 132.74, 130.79, 121.74, 45.48, 33.30, 28.68, 28.21, 25.74, 25.37, 25.07, 24.54, 22.39, 21.77; HRMS *m/z* calcd for $[M+H]^+$ $C_{17}H_{25}N_4O_2S$: 349.1693, found: 349.1685.

4.1.5. *General procedure for the synthesis of 4-{[2-(4-Oxo-5,6,7,8-Tetrahydro-3H-benzo[4,5]thieno[2,3-d] pyrimidin-3-yl)chloroacetyl] amino and aminomethyl} benzoic acid VIIIa and VIIIb*

A mixture of **II** (2.06 g, 10 mmol), anhydrous potassium carbonate (5.52 g, 40 mmol), 4-(2-chloroacetamido)benzoic acid **VIIa** or 4-[(2-chloroacetamido)methyl]benzoic acid **VIIb** (10 mmol) in 50 mL acetonitrile/water (1:1) was refluxed overnight. After acidification of the reaction mixture with hydrochloric acid (2 N), the resulting precipitate was collected by filtration, washed with water, dried and recrystallized from appropriate solvent to give the desired compounds **VIIIa** and **VIIIb** as white powder.

4.1.5.1. *4-{[2-(4-Oxo-5,6,7,8-Tetrahydro-3H-benzo[4,5]thieno[2,3-d]pyrimidin-3-yl) chloroacetyl]amino}benzoic acid (VIIIa)*. White powder (isopropanol), (2.57 g, 67% yield); mp: > 300 °C; IR (KBr, cm^{-1}): 3538, 3463, 3323, 3292 (NH, OH), 1667 (C═O) cm^{-1}. ^{1}H NMR (400 MHz, DMSO-d_6) δ (ppm): 12.74 (s, 1H, OH), 10.76 (s, 1H, NH), 8.31 (s, 1H, Ar-H), 7.91 (d, 2H, J = 8 Hz, Ar-H), 7.70 (d, 2H, J = 8 Hz, Ar-H), 4.86 (s, 2H, N−CH_2), 2.86 (t, 2H, J = 8 Hz, CH_2), 2.75 (t, 2H, J = 8 Hz, CH_2), 1.84–1.73 (m, 4H, 2 CH_2); ^{13}C NMR (100 MHz, DMSO-d_6) δ (ppm): 166.84, 165.93, 161.77, 156.92, 148.10, 142.56, 133.10, 130.79, 130.52, 125.53, 121.64, 118.37, 48.54, 25.30, 24.54, 22.40, 21.75; HRMS *m/z* calcd for $[M+H]^+$ $C_{19}H_{18}N_3O_4S$: 384.1013, found: 384.1005.

4.1.5.2. *4-{[2-(4-Oxo-5,6,7,8-Tetrahydro-3H-benzo[4,5]thieno[2,3-d] pyrimidin-3-yl)-chloroacetyl]aminomethyl}benzoic acid (VIIIb)*. White powder (DMF/H_2O), (2.47 g, 62% yield); mp: 293–295 °C; IR (KBr, cm^{-1}): 3316 (NH, OH), 1702 (C═O), 1678 (C═O) cm^{-1}. ^{1}H NMR (400 MHz, DMSO-d_6) δ (ppm): 12.90 (s, 1H, OH), 8.86 (t, 1H, J = 5.9 Hz, NH), 8.27 (s, 1H, Ar-H), 7.90 (d, 2H, J = 8 Hz, Ar-H), 7.40 (d, 2H, J = 8 Hz, Ar-H), 4.69 (s, 2H, N−CH_2), 4.39 (d, 2H, J = 5.9 Hz, NH−$C\underline{H}_2$), 2.87 (t, 2H, J = 8 Hz, CH_2), 2.75 (t, 2H, J = 8 Hz, CH_2), 1.83–1.74 (m, 4H, 2 CH_2); HRMS *m/z* calcd for $[M+H]^+$ $C_{20}H_{20}N_3O_4S$: 398.1169, found: 398.1159.

4.1.6. *General procedure for the synthesis of N-Hydroxy-4-{[2-(4-oxo-5,6,7,8-Tetrahydro-3H-benzo[4,5]thieno[2,3-d]pyrimidin-3-yl) chloroacetyl]amino or aminomethyl}benzamide IXa and IXb*

To a suspension of compound **VIIIa** or **VIIIb** (2.5 mmol) in acetonitrile (30 mL), Et_3N (0.87 mL, 6.25 mmol) was added. After cooling the reaction mixture to 0–5 °C, $ClCO_2C_2H_5$ (0.28 mL, 3 mmol) was

added drop wisely and the reaction mixture was stirred for further 30 mins at 0–5 °C. The reaction mixture was filtered and the filtrate was dropped into a freshly prepared solution of NH_2OH (1.74 g, 25 mmol) in methanol (10 mL). After stirring at room temperature for 1 h, the reaction mixture was quenched with water and the formed precipitate was filtered off, washed with water, dried and recrystallized from specified solvent to afford the target compounds **IXa** and **IXb**.

4.1.6.1. ***N-Hydroxy-4-{[2-(4-oxo-5,6,7,8-Tetrahydro-3H-benzo[4,5]thieno[2,3-d] (pyrimidin-3-yl)chloroacetyl]amino}benzamide (IXa)***. White powder (DMF/H_2O), (0.42 g, 42% yield); mp: 285–287 °C; IR (KBr, cm^{-1}): 3564, 3491, 3277 (NHOH), 1705 (C═O) cm^{-1}. ^{1}H NMR (400 MHz, DMSO-d_6) δ (ppm):11.22 (s, 1H, NH),10.89 (s, 1H, OH),8.87 (s, 1H, NH), 8.32 (s, 1H, Ar-H), 7.73 (d, 2H, J = 8 Hz, Ar-H), 7.67 (d, 2H, J = 8 Hz, Ar-H), 4.88 (s, 2H, N—CH_2), 2.87 (t, 2H, J = 8 Hz, CH_2), 2.75 (t, 2H, J = 8 Hz, CH_2), 1.83–1.74 (m, 4H,2 CH_2);^{13}C NMR (100 MHz, DMSO-d_6) δ (ppm):165.80, 161.76, 156.92, 148.15, 141.19, 133.06, 130.79, 130.46, 127.82, 127.51, 121.65, 118.34, 48.51, 45.36, 25.31, 24.55, 22.41, 21.76; HRMS *m/z* calcd for $[M+H]^+$ $C_{19}H_{19}N_4O_4S$: 399.1122, found: 399.1120.

4.1.6.2. ***N-Hydroxy-4-{[2-(4-oxo-5,6,7,8-Tetrahydro-3H-benzo[4,5]thieno[2,3-d] pyrimidin-3-yl)chloroacetyl]aminomethyl}benzamide (IXb)***. White powder (isopropanol), (0.45 g, 44% yield); mp: 218–220 °C; IR (KBr, cm^{-1}): 3486, 3309, 3201 (NHOH), 1654 (C═O) cm^{-1}. ^{1}H NMR (400 MHz, DMSO-d_6) δ (ppm): 11.20 (s, 1H, NH), 9.02 (s, 1H, OH), 8.84 (t, 1H, J = 5.9 Hz, NH), 8.27 (s, 1H, Ar-H), 7.72 (d, 2H, J = 8 Hz, Ar-H), 7.35 (d, 2H, J = 8 Hz, Ar-H), 4.69 (s, 2H, *N*-3-CH_2), 4.36 (d, 2H, J = 5.8 Hz, NH—CH_2), 2.87 (t, 2H, J = 8 Hz, CH_2), 2.75 (t, 2H, J = 8 Hz, CH_2), 1.82–1.73 (m, 4H, 2 CH_2); HRMS *m/z* calcd for $[M+H]^+C_{20}H_{21}N_4O_4S$: 413.1278, found: 413.1266.

4.1.7. General procedure for the synthesis of N-(2-Aminophenyl)-4-{[2-(4-oxo-5,6,7,8-Tetrahydro-3H-benzo[4,5]thieno[2,3-d]pyrimidin-3-yl) chloroacetyl]amino or aminomethyl} benzamide ***Xa*** *and* ***Xb***

To a suspension of compound **VIIIa** or **VIIIb** (2.5 mmol) in acetonitrile (30 mL), Et_3N (0.87 mL, 6.25 mmol) was added. After cooling the reaction mixture to 0–5 °C, $ClCO_2C_2H_5$ (0.28 mL, 3 mmol) was added drop wisely and the reaction mixture was stirred for further 30 mins at 0–5 °C. The reaction was filtered and the filtered was dropped into a solution of *o*-phenylenediamine (2.23 g, 20.62 mmol) in acetonitrile. After overnight stirring at room temperature, the reaction mixture was quenched by water and the separated solid was filtered off, washed with water and dried to afford the target compounds **Xa** and **Xb**.

4.1.7.1. ***N-(2-Aminophenyl)-4-{[2-(4-oxo-5,6,7,8-Tetrahydro-3H-benzo[4,5] thieno[2,3-d]pyrimidin-3-yl)chloroacetyl]amino}benzamide (Xa)***. White powder (DMF/H_2O), (1.03 g, 87% yield); mp: > 300 °C; IR (KBr, cm^{-1}): 3465, 3312, 3215 (NH, NH_2), 1668 (C═O) cm^{-1}. ^{1}H NMR (400 MHz, DMSO-d_6) δ (ppm): 10.73 (s, 1H, NH), 9.60 (s, 1H, NH), 8.32 (s, 1H, Ar-H), 7.98 (d, 2H, J = 8.6 Hz, Ar-H), 7.71 (d, 2H, J = 8.6 Hz, Ar-H), 7.17 (d, 1H, J = 7.9 Hz, Ar-H), 6.97 (t, 1H, J = 7.6 Hz, Ar-H), 6.78 (d, 1H, J = 8 Hz, Ar-H), 6.60 (t, 1H, J = 7.6 Hz, Ar-H), 4.89 (s, 2H, NH_2), 4.88 (s, 2H, N—CH_2), 2.86 (t, 2H, J = 8 Hz, CH_2), 2.75 (t, 2H, J = 8 Hz, CH_2), 1.83–1.73 (m, 4H,2 CH_2); ^{13}C NMR (100 MHz, DMSO-d_6) δ (ppm): 165.82, 164.65, 161.79, 156.95, 148.11, 143.15, 141.34, 133.11, 130.79, 129.37, 128.86, 126.68, 126.40, 123.43, 121.65, 118.21, 116.27, 116.13, 48.50, 25.33, 24.55, 22.41, 21.77; HRMS *m/z* calcd for $[M+H]^+$ $C_{25}H_{24}N_5O_3S$: 474.1594, found: 474.1596.

4.1.7.2. ***N-(2-Aminophenyl)-4-{[2-(4-oxo-5,6,7,8-Tetrahydro-3H-benzo[4,5] thieno[2,3-d]pyrimidin-3-yl)chloroacetyl]aminomethyl} benzamide (Xb)***. White powder (DMF/H_2O), (0.88 g, 72% yield); mp: 238–239 °C; IR (KBr, cm^{-1}): 3469, 3323, 3219 (NH, NH_2), 1678 (C═O) cm^{-1}. ^{1}H NMR (400 MHz, DMSO-d_6) δ (ppm): 9.66 (s, 1H, NH), 8.90 (t, 1H, J = 6 Hz, NH), 8.29 (s, 1H, Ar-H), 7.97 (d, 2H, J = 7.9 Hz, Ar-H), 7.43 (d, 2H, J = 7.9 Hz, Ar-H), 7.20 (d, 1H, J = 7.9 Hz, Ar-H), 6.99 (t, 1H, J = 7.6 Hz, Ar-H), 6.81 (d, 1H, J = 8 Hz, Ar-H), 6.62 (t, 1H, J = 7.6 Hz, Ar-H), 4.94 (s, 2H, NH_2), 4.72 (s, 2H, *N*-3-CH_2), 4.42 (d, 2H, J = 5.9 Hz, NH—CH_2), 2.88 (t, 2H, J = 8 Hz, CH_2), 2.75 (t, 2H, J = 8 Hz, CH_2), 1.81–1.75 (m, 4H,2 CH_2); HRMS *m/z* calcd for $[M+H]^+$ $C_{26}H_{26}N_5O_3S$: 488.1751, found: 488.1737.

4.1.8. ***General procedure for the synthesis of 4-{[2-(4-Oxo-5,6,7,8-Tetrahydro-3H-benzo[4,5]thieno[2,3-d]pyrimidin-3-yl)chloroacetyl] amino}benzoic acid hydrazide XIa*** *and* ***XIb***

To a solution of compound **VIIIa** or **VIIIb** (2.5 mmol) in acetonitrile (30 mL), Et_3N (0.87 mL, 6.25 mmol) was added. After cooling the reaction mixture to 0–5 °C, $ClCO_2C_2H_5$ (0.28 mL, 3 mmol) was added drop wisely and the reaction mixture was stirred for further 30 min at 0–5 °C. The reaction mixture was filtered and the filtrate was dropped into a solution of hydrazine hydrate (0.5 mL, 10 mmol) in acetonitrile. After stirring at room temperature overnight, the reaction mixture was quenched by water and the formed precipitate was filtered off, washed with water and cold ethanol and dried to afford the target compounds **XIa** and **XIb**.

4.1.8.1. ***4-{[2-(4-Oxo-5,6,7,8-Tetrahydro-3H-benzo[4,5]thieno[2,3-d]pyrimidin-3-yl)chloroacetyl]amino}benzoic acid hydrazide (XIa)***. White powder (DMF/H_2O), (0.81 g, 81% yield); mp: 293–295 °C; IR (KBr, cm^{-1}): 3318, 3225 (NH, NH_2), 1660 (C═O) cm^{-1}. ^{1}H NMR (400 MHz, DMSO-d_6) δ (ppm): 10.74 (s, 1H, NH), 9.67 (s, 1H, NH), 8.31 (s, 1H, Ar-H), 7.80 (d, 2H, J = 8.3 Hz, Ar-H), 7.64 (d, 2H, J = 8.3 Hz, Ar-H), 4.86 (s, 2H, N—CH_2), 4.44 (s, 2H, NH_2), 2.86 (t, 2H, J = 8 Hz, CH_2), 2.75 (t, 2H, J = 8 Hz, CH_2), 1.80–1.73 (m, 4H,2 CH_2); ^{13}C NMR (100 MHz, DMSO-d_6) δ (ppm): 170.23, 166.09, 161.65, 156.83, 148.39, 148.13, 142.96, 132.86, 132.65, 130.77, 121.63, 109.55, 46.41, 25.31, 24.53, 22.41, 21.76; HRMS *m/z* calcd for $[M+H]^+$ $C_{19}H_{20}N_5O_3S$: 398.1281, found: 398.1270.

4.1.8.2. ***4-{[2-(4-Oxo-5,6,7,8-Tetrahydro-3H-benzo[4,5]thieno[2,3-d]pyrimidin-3-yl)chloroacetyl]aminomethylbenzoic acid hydrazide (XIb)***. White powder (DMF/H_2O), (0.80 g, 78% yield); mp: 260–262 °C; IR (KBr, cm^{-1}): 3312, 3255 (NH, NH_2), 1656 (C═O) cm^{-1}; ^{1}H NMR (400 MHz, DMSO-d_6) δ (ppm): 9.74 (s, 1H, NH), 8.83 (t, 1H, J = 6 Hz, NH), 8.27 (s, 1H, Ar-H), 7.78 (d, 2H, J = 7.9 Hz, Ar-H), 7.34 (d, 2H, J = 7.9 Hz, Ar-H), 4.69 (s, 2H, *N*-3-CH_2), 4.55 (s, 2H, NH_2), 4.36 (d, 2H, J = 5.9 Hz, NH—CH_2), 2.87 (t, 2H, J = 8 Hz, CH_2), 2.75 (t, 2H, J = 8 Hz, CH_2), 1.82–1.76 (m, 4H, 2 CH_2); HRMS *m/z* calcd for $[M+H]^+$ $C_{20}H_{22}N_5O_3S$: 412.1438, found: 412.1426.

4.2. Biology

4.2.1. ***HDAC inhibitory activity assays***

The HDAC inhibitory activity of final compounds was measured using Color-de-Lys™ HDAC Colorimetric Assay/Drug Discovery Kit (BML-AK501-0001, Enzo Life Sciences, Inc.) following the protocol provided by the supplier [39–41]. **See Appendix A.**

4.2.2. ***In vitro anti-proliferative assays***

All cell lines were maintained in RPMI1640 medium containing 10% FBS at 37 °C in 5% CO_2 humidified incubator. Cell proliferation assay was determined by the MTT (3-[4,5-dimethyl-2-thiazolyl]-2,5-diphenyl-2H-tetrazolium bromide) method [36]. **See Appendix A.**

4.2.3. HDAC isoforms inhibitory activity

All of the enzymatic reactions for HDAC1, HDAC2, HDAC6 and HDAC8 were conducted at 37 °C for 30 mins [42]. **See Appendix A.**

4.2.4. Cell cycle analysis

Cell cycle analysis was performed on PC3cell line after treatment with compounds **IVb** and **IXb** [43]. **See Appendix A.**

4.2.5. Apoptotic assay

Apoptotic assay was performed on PC3cell line after treatment with compounds **IVb** and **IXb** [2]. **See Appendix A.**

4.3. Docking methodology

Discovery Studio 2.5 software (Accelrys Inc., San Diego, CA, USA) was used for docking analysis. Fully automated docking tool using "Dock ligands (CDOCKER)" protocol running on Intel (R) core (TM) i32370 CPU @ 2.4 GHz 2.4 GHz, RAM Memory 2 GB under the Windows 7.0 system. The crystal structure of known HDAC2 inhibitor Vorinostat (SAHA, **1**) in complex with HDAC2 (**PDB: 4LXZ**) was downloaded from protein data bank [37]. **See Appendix A.**

Appendix A

A.1 Biological evaluation

A.1.1. *HDAC inhibitory activity assays*

The HDAC inhibitory activity of final compounds was measured using Color-de-Lys™ HDAC Colorimetric Assay/Drug Discovery Kit (BML-AK501-0001, Enzo Life Sciences, Inc.) following the protocol provided by the supplier [29–31]. The kit is useful for inhibitors screening using HDAC from HeLa nuclear extract. The *Color de Lys*™ substrate, which comprises an acetylated lysine, is incubated with sample containing HDAC activity. Deacetylation of the substrate sensitizes the substrate. The mixing with the *Color de Lys*™ developer causes an increase in color intensity at 405 nm.

The tested compounds and SAHA were diluted in buffer to a concentration of 1.25 μM. HDACs (5 μL) and incubated at 37 °C with 10 μL of compounds and 25 μL of substrate on 96-well plates. After incubation for 30 min, *Color de Lys*™ developer (50 μL/well) was added to stop HDAC reactions. Incubate plate at37 °C for 15 min. at the end of incubation period, read the plate in microtiter-plate reader at 405 nm. The optical density values are indicative of the HDAC inhibitory activity for the tested compounds.

A.1.2. *In vitro anti-proliferative assays*

All cell lines were maintained in RPMI1640 medium containing 10% FBS at 37 °C in 5% CO_2 humidified incubator. Cell proliferation assay was determined by the MTT (3-[4,5-dimethyl-2-thiazolyl]-2,5-diphenyl-2H-tetrazolium bromide) method [32]. Briefly, cells were plated in triplicate wells (3–5 × 10^4 cells/well) of 96-well flat-bottomed plates and incubated overnight prior to drug exposure and then treated with different concentrations of the tested compounds for 48 h. After that, 20 μL of MTT reagent at a final concentration of 0.5 mg/mL was added to each well. Cells were then incubated for 2 h with MTT, after which 100 μL of DMSO solution was added to dissolve the formazan salt resulting from the reduction of MTT and the absorbance was read at 570 nm using an automatic plate reader [32]. The IC_{50} values were calculated according to inhibition ratios from three independent experiments.

A.1.3. HDAC isoform inhibitory activity

All of the enzymatic reactions were conducted at 37 °C for 30 min. The 50 mL reaction mixture contains 25 mM Tris, pH 8.0, 1 mM MgCl2, 0.1 mg/ml BSA, 137 mM NaCl, 2.7 mM KCl, HDAC and the enzyme substrate. The compounds were diluted in 10% DMSO and 5 mL of the dilution was added to a 50 mL reaction so that the final concentration of DMSO is 1% in all of reactions. The assay was performed by quantitating the fluorescent product amount of in solution following an enzyme reaction. Fluorescence is then analyzed with an excitation of 350e360 nm and an emission wavelength of 450e460 nm at SpectraMax M5 microtiter plate reader. The IC50 values were calculated using nonlinear regression with normalized dose-response fit in Prism GraphPad software [35].

A.1.4. Cell cycle analysis

Cell cycle analysis PC3 cell was seeded into six-well plates at a density of 2 × 10^5 cell per well and incubated for 24 h. The cell was cultured in RPMI 1640 supplemented with fetal bovine serum (FBS, 10%) and incubated at 37 °C and 5% CO_2. The medium was removed and replaced with medium (final DMSO concentration, 1% v/v) containing compounds IVb and IXb (0.067 and 0.027 μM). After incubation for 24 h and 48 h, the cell layer was trypsinized and washed with cold phosphate buffered saline (PBS) and fixed with 70% ethanol. The fixed cells were rinsed with PBS and then stained with the DNA fluorochrome PI in a solution containing Triton X-100 as well as RNase, keep 15 min at 37 °C according the instruction manual. Then the samples were analyzed with a FACS Caliber flow cytometer (Becton Dickinson & Co., Franklin Lakes, NJ). The number of cells analyzed for each sample was 10,000 [36].

A.1.5. Apoptosis assay

The PC3 was treated with 1.4 μM of compound **IVb** and 0.4 μM of compound **IXb** for 24 h. After treatment, the cells were suspended in 0.5 mL of PBS, collected by centrifugation, and fixed in ice-cold 70% (v/v) ethanol, centrifuged the ethanol-suspended cells for 5 min, suspended in 5 mL PBS and centrifuged for 5 min, re-suspended with 1 mL PI staining solution (0.1 mg/ml RNase) + PE Annexin V (component no. 51-65875X) and kept in dark at 37 °C for 10 min, finally analyzed by flow cytometry using FACS caliber (Becton Dickinson). The cell cycle distributions were calculated using Phoenix Flow Systems and Verity Software House [36].

A.2. Docking methodology

Discovery Studio 2.5 software (Accelrys Inc., San Diego, CA, USA) was used for docking analysis. Fully automated docking tool using "Dock ligands (CDOCKER)" protocol running on Intel (R) core (TM) i32370 CPU @ 2.4 GHz 2.4 GHz, RAM Memory 2 GB under the Windows 7.0 system. The crystal structure of known HDAC2 inhibitor Vorinostat (SAHA, **1**) in complex with HDAC2 (PDB: 4LXZ) was downloaded from protein data bank [1]. The docked compounds were built using Chem. 3D ultra 12.0 software [Chemical Structure Drawing Standard; Cambridge Soft corporation, USA (2010)], and copied to Discovery Studio 2.5 software. Automatic protein preparation module was used applying CHARMm forcefield. The binding site sphere has been defined automatically by the software. Now the above prepared receptor is given as input for "input receptor molecule" parameter in the CDOCKER protocol parameter explorer. Force fields are applied on compounds IVa, IVb, IXa and IXb to get the minimum lowest energy structure. The obtained poses were studied and the poses showing best ligand–HDAC interactions were selected and used for CDOCKER energy (protein-ligand interaction energies) calculations. Receptor–ligand interactions of the complexes were examined in 2D and 3D styles

References

[1] M.F.A. Mohamed, M.S.A. Shaykoon, M.H. Abdelrahman, B.E.M. Elsadek, A.S. Aboraia, G. Abuo-Rahma, Design, synthesis, docking studies and biological evaluation of novel chalcone derivatives as potential histone deacetylase inhibitors, Bioorg. Chem. 72 (2017) 32–41.
[2] M.S. Abdelbaset, G.E.A. Abuo-Rahma, M.H. Abdelrahman, M. Ramadan, B.G.M. Youssif, S.N.A. Bukhari, M.F.A. Mohamed, M. Abdel-Aziz, Novel pyrrol-2(3H)-ones and pyridazin-3(2H)-ones carrying quinoline scaffold as anti-proliferative tubulin polymerization inhibitors, Bioorg. Chem. 80 (2018) 151–163.
[3] C. Balch, J.S. Montgomery, H.I. Paik, S. Kim, T.H. Huang, K.P. Nephew, New anti-cancer strategies: epigenetic therapies and biomarkers, Front. Biosci. 10 (2005) 1897–1931.
[4] P.A. Jones, S.B. Baylin, The fundamental role of epigenetic events in cancer, Nat. Rev. Genet. 3 (2002) 415–428.
[5] K.J. Falkenberg, R.W. Johnstone, Histone deacetylases and their inhibitors in cancer, neurological diseases and immune disorders, Nat. Rev. Drug Discovery 13 (2014) 673–691.
[6] D. Son, C.S. Kim, K.R. Lee, H.J. Park, Identification of new quinic acid derivatives as histone deacetylase inhibitors by fluorescence-based cellular assay, Bioorg. Med.

Chem. Lett. 26 (2016) 2365–2369.
[7] P.A. Marks, The clinical development of histone deacetylase inhibitors as targeted anticancer drugs, Expert Opin. Investig. Drugs 19 (2010) 1049–1066.
[8] P.A. Marks, W.S. Xu, Histone deacetylase inhibitors: potential in cancer therapy, J. Cell Biochem. 107 (2009) 600–608.
[9] M. Mottamal, S. Zheng, T.L. Huang, G. Wang, Histone deacetylase inhibitors in clinical studies as templates for new anticancer agents, Molecules 20 (2015) 3898–3941.
[10] K.P. Garnock-Jones, Panobinostat: first global approval, Drugs 75 (2015) 695–704.
[11] M. Guha, HDAC inhibitors still need a home run, despite recent approval, Nat. Rev. Drug Discov. 14 (2015) 225–226.
[12] N.S. Habib, R. Soliman, A.A. El-Tombary, S.A. El-Hawash, O.G. Shaaban, Synthesis and biological evaluation of novel series of thieno[2,3-d]pyrimidine derivatives as anticancer and antimicrobial agents, Med. Chem. Res. 22 (2013) 3289–3308.
[13] M. Modica, M. Santagati, A. Santagati, V. Cutuli, N. Mangano, A. Caruso, Synthesis of new [1,3,4]thiadiazolo[3,2-a]thieno[2,3-d]pyrimidinone derivatives with anti-inflammatory activity, Pharmazie 55 (2000) 500–502.
[14] M.M. el-Kerdawy, M.Y. Yousif, A.A. el-Emam, M.A. Moustafa, M.A. el-Sherbeny, Synthesis and antiinflammatory activity of certain thienopyrimidine derivatives, Boll Chim. Farmaceutico 135 (1996) 301–305.
[15] R.V. Chambhare, B.G. Khadse, A.S. Bobde, R.H. Bahekar, Synthesis and preliminary evaluation of some N-[5-(2-furanyl)-2-methyl-4-oxo-4H-thieno[2,3-d]pyrimidin-3-yl]-carboxamide and 3-substituted-5-(2-furanyl)-2-methyl-3H-thieno[2,3-d]pyrimidin-4-ones as antimicrobial agents, Eur. J. Med. Chem. 38 (2003) 89–100.
[16] M.B. Devani, C.J. Shishoo, U.S. Pathak, S.H. Parikh, G.F. Shah, A.C. Padhya, Synthesis of 3-substituted thieno [2, 3-d] pyrimidin-4(3H)-one-2-mercaptoacetic acids and their ethyl esters for pharmacological screening, J. Pharm. Sci. 65 (1976) 660–664.
[17] N.A. Santagati, A. Caruso, V.M. Cutuli, F. Caccamo, Synthesis and pharmacological evaluation of thieno[2,3-d]pyrimidin-2,4-dione and 5H-pyrimido [5,4-b]indol-2,4-dione derivatives, Farmaco 50 (1995) 689–695.
[18] L.D. Jennings, S.L. Kincaid, Y.D. Wang, G. Krishnamurthy, C.F. Beyer, J.P. McGinnis, M. Miranda, C.M. Discafani, S.K. Rabindran, Parallel synthesis and biological evaluation of 5,6,7,8-tetrahydrobenzothieno[2,3-d]pyrimidin-4(3H)-one cytotoxic agents selective for p21-deficient cells, Bioorg. Med. Chem. Lett. 15 (2005) 4731–4735.
[19] M.S. Manhas, S.D. Sharma, S.G. Amin, Heterocyclic compounds. 4. Synthesis and antiinflammatory activity of some substituted thienopyrimidones, J. Med. Chem. 15 (1972) 106–107.
[20] M.J. Munchhof, J.S. Beebe, J.M. Casavant, B.A. Cooper, J.L. Doty, R.C. Higdon, S.M. Hillerman, C.I. Soderstrom, E.A. Knauth, M.A. Marx, A.M. Rossi, S.B. Sobolov, J. Sun, Design and SAR of thienopyrimidine and thienopyridine inhibitors of VEGFR-2 kinase activity, Bioorg. Med. Chem. Lett. 14 (2004) 21–24.
[21] Y.D. Wang, S. Johnson, D. Powell, J.P. McGinnis, M. Miranda, S.K. Rabindran, Inhibition of tumor cell proliferation by thieno[2,3-d]pyrimidin-4(1H)-one-based analogs, Bioorg. Med. Chem. Lett. 15 (2005) 3763–3766.
[22] H. Amawi, C. Karthikeyan, R. Pathak, N. Hussein, R. Christman, R. Robey, C.R. Ashby Jr., P. Trivedi, A. Malhotra, A.K. Tiwari, Thienopyrimidine derivatives exert their anticancer efficacy via apoptosis induction, oxidative stress and mitotic catastrophe, Eur. J. Med. Chem. 138 (2017) 1053–1065.
[23] E.Z. Elrazaz, R.A.T. Serya, N.S.M. Ismail, D.A. Abou El Ella, K.A.M. Abouzid, Thieno [2,3-d]pyrimidine based derivatives as kinase inhibitors and anticancer agents, Future J. Pharm. Sci. 1 (2015) 33–41.
[24] C.-H. Wu, M.S. Coumar, C.-Y. Chu, W.-H. Lin, Y.-R. Chen, C.-T. Chen, H.-Y. Shiao, S. Rafi, S.-Y. Wang, H. Hsu, C.-H. Chen, C.-Y. Chang, T.-Y. Chang, T.-W. Lien, M.-Y. Fang, K.-C. Yeh, C.-P. Chen, T.-K. Yeh, S.-H. Hsieh, J.T.A. Hsu, C.-C. Liao, Y.-S. Chao, H.-P. Hsieh, Design and synthesis of tetrahydropyridothieno[2,3-d]pyrimidine scaffold based epidermal growth factor receptor (EGFR) kinase inhibitors: the role of side chain chirality and michael acceptor group for maximal potency, J. Med. Chem. 53 (2010) 7316–7326.
[25] Y.C. Mayur, G.J. Peters, V.V. Prasad, C. Lemo, N.K. Sathish, Design of new drug molecules to be used in reversing multidrug resistance in cancer cells, Curr. Cancer Drug Targets 9 (2009) 298–306.
[26] V.R. Solomon, C. Hu, H. Lee, Hybrid pharmacophore design and synthesis of isatin-benzothiazole analogs for their anti-breast cancer activity, Bioorg. Med. Chem. 17 (2009) 7585–7592.
[27] K. Gewald, E. Schinke, H. Bottcher, Heterocyclen aus CH-aciden Nitrilen, VIII. 2-Amino-thiophene aus methylenaktiven Nitrilen, Carbonylverbindungen und Schwefel, Chem. Ber. 99 (1996) 94–100.
[28] F.E. El-Baih, H.A. Al-Blowy, H.M. Al-Hazimi, Synthesis of some thienopyrimidine derivatives, Molecules 11 (2006) 498–513.
[29] R. Ragno, A. Mai, S. Massa, I. Cerbara, S. Valente, P. Bottoni, R. Scatena, F. Jesacher, P. Loidl, G. Brosch, 3-(4-Aroyl-1-methyl-1H-pyrrol-2-yl)-N-hydroxy-2-propenamides as a new class of synthetic histone deacetylase inhibitors. 3. Discovery of novel lead compounds through structure-based drug design and docking studies, J. Med. Chem. 47 (2004) 1351–1359.
[30] A. Mai, S. Massa, I. Cerbara, S. Valente, R. Ragno, P. Bottoni, R. Scatena, P. Loidl, G. Brosch, 3-(4-Aroyl-1-methyl-1H-2-pyrrolyl)-N-hydroxy-2-propenamides as a new class of synthetic histone deacetylase inhibitors. 2. Effect of pyrrole-C2 and/or -C4 substitutions on biological activity, J. Med. Chem. 47 (2004) 1098–1109.
[31] A.J. Harte, T. Gunnlaugsson, Synthesis of alpha-chloroamides in water, Tetrahedron Lett. 47 (2006) 6321–6324.
[32] J. Qiu, B. Xu, Z. Huang, W. Pan, P. Cao, C. Liu, X. Hao, B. Song, G. Liang, Synthesis and biological evaluation of Matijing-Su derivatives as potent anti-HBV agents, Bioorg. Med. Chem. 19 (2011) 5352–5360.
[33] M. Suchy, M. Milne, A.A. Elmehriki, N. McVicar, A.X. Li, R. Bartha, R.H. Hudson, Introduction of peripheral carboxylates to decrease the charge on Tm(3+) DOTAM-Alkyl complexes: implications for detection sensitivity and in vivo toxicity of PARACEST MRI contrast agents, J. Med. Chem. 58 (2015) 6516–6532.
[34] E.H. Zhang, R.F. Wang, S.Z. Guo, B. Liu, An update on antitumor activity of naturally occurring chalcones, Evid. Based Complement. Alternat. Med. 2013 (2013) 815621.
[35] Y. Huang, M. Tan, M. Gosink, K.K. Wang, Y. Sun, Histone deacetylase 5 is not a p53 target gene, but its overexpression inhibits tumor cell growth and induces apoptosis, Cancer Res. 62 (2002) 2913–2922.
[36] S.B. Sobottka, M.R. Berger, Assessment of antineoplastic agents by MTT assay: partial underestimation of antiproliferative properties, Cancer Chemother. Pharmacol. 30 (1992) 385–393.
[37] B.E. Lauffer, R. Mintzer, R. Fong, S. Mukund, C. Tam, I. Zilberleyb, B. Flicke, A. Ritscher, G. Fedorowicz, R. Vallero, D.F. Ortwine, J. Gunzner, Z. Modrusan, L. Neumann, C.M. Koth, P.J. Lupardus, J.S. Kaminker, C.E. Heise, P. Steiner, Histone deacetylase (HDAC) inhibitor kinetic rate constants correlate with cellular histone acetylation but not transcription and cell viability, J. Biol. Chem. 288 (2017) 26926–26943.
[38] D. Briel, A. Rybak, C. Kronbach, K. Unverferth, Substituted 2-aminothiopen-derivatives: a potential new class of GluR6-antagonists, Eur. J. Med. Chem. 45 (2010) 69–77.
[39] X. Qu, M. Proll, C. Neuhoff, R. Zhang, M.U. Cinar, M.M. Hossain, D. Tesfaye, C. Grosse-Brinkhaus, D. Salilew-Wondim, E. Tholen, C. Looft, M. Holker, K. Schellander, M.J. Uddin, Sulforaphane epigenetically regulates innate immune responses of porcine monocyte-derived dendritic cells induced with lipopolysaccharide, PLoS ONE 10 (2015) e0121574.
[40] W. Lu, F. Wang, T. Zhang, J. Dong, H. Gao, P. Su, Y. Shi, J. Zhang, Search for novel histone deacetylase inhibitors. Part II: design and synthesis of novel isoferulic acid derivatives, Bioorg. Med. Chem. 22 (2014) 2707–2713.
[41] F. Wang, W. Lu, T. Zhang, J. Dong, H. Gao, P. Li, S. Wang, J. Zhang, Development of novel ferulic acid derivatives as potent histone deacetylase inhibitors, Bioorg. Med. Chem. 21 (2013) 6973–6980.
[42] C. Chen, X. Hou, G. Wang, W. Pan, X. Yang, Y. Zhang, H. Fang, Design, synthesis and biological evaluation of quinoline derivatives as HDAC class I inhibitors, Eur. J. Med. Chem. 133 (2017) 11–23.
[43] H.A.M. El-Sherief, B.G.M. Youssif, S.N. Abbas Bukhari, A.H. Abdelazeem, M. Abdel-Aziz, H.M. Abdel-Rahman, Synthesis, anticancer activity and molecular modeling studies of 1,2,4-triazole derivatives as EGFR inhibitors, Eur. J. Med. Chem. 156 (2018) 774–789.